1-1-1975

Fatigue strength of tack welded tie plates.

Donald P. Erb

FATIGUE STRENGTH OF

TACK WELDED TIE PLATES

by

Donald P. Erb

A THESIS

Presented to the Graduate Committee

of Lehigh University

in Candidacy for the Degree of

Master of Science

in

Civil Engineering

Lehigh University

September 1975

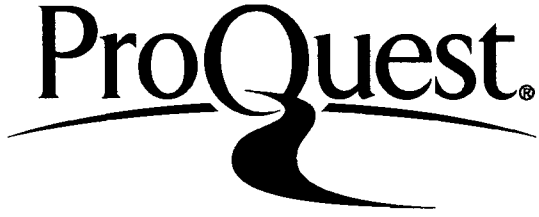

This thesis is accepted and approved in partial fulfillment of the requirements for the degree of Master of Science.

Sept. 15, 1975
(date)

Professor John W. Fisher

Professor David A. VanHorn
Chairman, Department of Civil Engineering

ACKNOWLEDGMENTS

This investigation was part of PennDOT Research Project 72-3, High Cycle Fatigue of Welded Bridge Details. The testing program was conducted at Fritz Engineering Laboratory, Lehigh University. Dr. Lynn S. Beedle is the Director of Fritz Engineering Laboratory and Dr. David A. VanHorn is the Chairman of the Civil Engineering Department.

The specimens were fabricated in the machine shop of Fritz Engineering Laboratory. Mr. Richard N. Sopko prepared the photographs. The manuscript was typed by Mrs. Ruth Grimes.

Thanks are also due Dr. John W. Fisher for his supervision and suggestions during the preparations of this manuscript and Mr. Nicholas Zettlemoyer for his assistance in the finite element phase of the investigation.

TABLE OF CONTENTS

LIST OF TABLE AND FIGURES

ABSTRACT

Fatigue cracks have been discovered in tie plates on several bridges. These plates connect the outrigger bracket to the longitudinal girder and floor beam. On the Lehigh Canal Bridge the cracks were observed to grow from the ends of tack welds placed on the tie plate edges adjacent to the cantilever bracket. Since fatigue test data for this type of geometrical configuration was not available, a series of tie plates were tested to acquire the needed data. From this data it was found that AASHTO Category D provides a reaonable estimate of the lower bound fatigue strength of this detail.

In conjunction with the physical testing, an analytical study of crack growth in the tie plates was undertaken to confirm the experimental results. A finite element analysis was used to calculate the stress concentration factor at the end of the weld. Two different stress concentration decay functions were used in the fracture mechanics analysis of crack growth and estimation of detail life under cyclic loading. Both functions gave reasonable estimates of the detail's lower bound fatigue strength.

1. INTRODUCTION

Tie plates on several bridges, including the Lehigh Canal Bridge, have developed fatigue cracks In the Lehigh Canal Bridge these cracks have grown from the end of tack welds (approximately 2 in. long) placed between the tie plate and the top flange of the outrigger bracket during construction of the bridge. The tack weld, in addition to providing the initial flaw from which the crack propagation, introduces a concentration of stress at the flaw location, thereby accelerating crack growth.

A complex interaction of several bridge members produces the cyclic stresses which drives the crack. The concrete slab, curb and parapet provide a relatively stiff in-plane system supported by the stringers (see Fig. 1). The stringers rest on the floor beams and outrigger bracket, with the outside stringer attached 6-1/4 in. from the end of the bracket. The outrigger bracket is attached to the longitudinal girder by the tie plate and a simple web angle connection, which offers little lateral restraint. The tie plates are continuous over the longitudinal girder, being connected to the floor beam, longitudinal girder and outrigger bracket with 7/8 in. rivets. This provides a relatively rigid connection at the girder.

As vehicles pass over the bridge, bending stresses develop in the longitudinal girders. Compressive stresses in the top flange of the girder in positive moment regions cause the top flange to

shorten when the vehicle is in the span. Smaller tensile stresses occur in the top flange when the vehicle is in the adjacent span. Since the bracket is attached by the outside stringer, to the relatively stiff deck slab, the cross-sectional rotation of the longitudinal girder at each floor beam - outrigger bracket during passage of vehicles over the bridge causes a relative displacement to develop between the top flange of the girder and the end of the outrigger bracket. This relative displacement produces in-plane bending moment stresses in the tie plate and top flange of the bracket thereby developing the cyclic stresses which result in fatigue crack growth.

Since the longitudinal girder is continuous over three spans, the girder is subjected to both positive and negative bending moments. Hence the tie plates experience various degrees of stress reversals as the top flange of the girder shortens or lengthens depending on the vehicle location along the bridge and the position of the tie plate[1].

Because of the cracked tie plates on the Lehigh Canal Bridge, it was desirable to have a laboratory definition of the fatigue strength of the tie plate. Fatigue test data were not available for the geometrical configuration that existed. To assist in defining the applicable stress range - cycle life relationship, a series of twenty tie plates were tested at various stress ranges on the dynamic test bed of Fritz Engineering Laboratory.

A second objective of this study was to confirm the experimental results with an analytical study of crack growth in the tie

plates. Since the origin of the fatigue crack was at the end of the tack weld, it was necessary to determine the stress concentration factor in order to calculate the stress intensity factor range experienced by the crack[2,3]. A finite element solution was used to estimate the stress concentration factor at the tack weld toe. Then the principles of fracture mechanics were used to analyze the growth of the crack.

2. DESCRIPTION OF TEST SPECIMEN

It was desirable to have the experimental tie plates duplicate the tie plates installed on the Lehigh Canal Bridge as much as possible. Two sizes of the plates are used on the bridge. Only sixteen 12 in. wide plates (12" x 3'-8" x 1/2") were used over the interior piers of the bridge. Two hundred 10 in. wide plates are used at other floor beam locations. Hence, the tie plate tested in the laboratory was modeled after the narrower plate, which is shown in Fig. 2.

Figure 3 shows the dimensions of the test specimens. By comparing with Fig. 2, it can be seen that the 10 in. width and 0.5 in. thickness of the test specimen was the same as the narrower bridge tie plate. Since the fatigue cracks grew from construction tack welds on the outrigger bracket side of the tie plate, it was not necessary to include the floor beam portion of the tie plate in the test specimen. Hence the test specimen was shortened from 3 ft.-8 in. to 2 ft.-0 in.

The hole pattern used for the tie plate - outrigger bracket connection was maintained. But, the hole pattern corresponding to the longitudinal girder - tie plate connection had to be altered to match the dynamic test bed's W12 x 85 column holes, to which the specimens were to be bolted. Fritz Engineering Laboratory did not have the equipment to drive 7/8 in. rivets, therefore bolts had to be used. One inch bolts were used as they were readily available and the

increased hole diameter did not appreciably alter the net area of the tie plate. The necessary 1-1/16 in. holes for the bolts were drilled instead of being punched as the 15/16 in. holes of the tie plates were. This change was not considered significant for two reasons. First, the fatigue cracks did not grow through the holes. Second, the end of the tack weld, where the fatigue crack originates, is just outside of the bolted connection between the tie plate and loading beam.

Because of the availability of plate material, plates were taken from the laboratory's stock. A total of thirteen specimens, marked as TPC-x were made out of mild steel. Six of these were cut from 1/2 in. plate that had been removed from a highway bridge. Another ten specimens were cut from 1/2 in. A514 steel plate. These are marked as TPC-x.

One other detail of the specimen fabrication should be mentioned. All edges were saw cut to ensure that there would be comparable discontinuities along the specimen's edges after the tack welds were placed.

3. TESTING APPARATUS AND TECHNIQUES

3.1 Installation of Tie Plates

Figure 4 shows the test setup used for the tie plate experiments. One end of the tie plate was bolted to the W12 x 85 column, while the other end was bolted to the W12 x 120 beam flange. The beam was loaded by a 22 kip Amsler hydraulic jack connected to an Amsler pulsator.

The tie plates were installed using the following procedure: the bolted connections were placed in bearing and the bolts were then torqued to develop between 20 - 25 kips preload, i.e. between 1/3 - 1/2 of specified preload. This was to simulate the clamping force in the rivets. Then the construction tack weld was placed.

The 3/16 in. construction tack welds were placed on both sides of the tie plate and varied in length and location. A field inspection of these welds indicated that they started about 1/2 in. from the end of the outrigger bracket top flange and had an average length of 2 in. Therefore, the laboratory tack weld was standardized in the test as a 3/16 in. weld starting 1/2 in. in from the end of the beam and extending 2 in. as shown in Fig. 4. This weld was placed on both sides of the tie plate as observed on the bridge structure.

3.2 Comparison of Test Setup to Bridge

Figures 1b and 4 provide a comparison between the test setup and the Lehigh Canal Bridge. The W12 x 85 column simulated one of the

bridge's longitudinal girders, while the flange of the W12 x 120 beam simulated the top flange of the outrigger bracket. In addition the 1/2 in. gap that existed between the longitudinal girder flange and the outrigger bracket top flange was duplicated as a 1/2 in gap between the column flange and the beam flange in the test setup.

On the bridge a stringer is attached to the end of the outrigger bracket at a distance of 2 ft.-6 in. from the edge of the longitudinal girder's top flange. Corresponding to the stringer, at 2 ft.-6 in. from the column flange of the test setup, a jack introduced a cyclic displacement of the end of the beam. This provided the same moment gradient in the tie plate as existed in the bridge due to the relative displacement of the longitudinal girder's top flange and the end of the outrigger bracket.

3.3 Testing Procedures

The stress in the tie plates was controlled by electrical strain gages attached to the plates. For the first set of the plates tested, TPC-1a and TPC-1b, the strain gages were placed on the face of the tie plates as shown in Fig. 5. There proximity to the bolted connection resulted in jack loads which were twice as large as was predicted from bending theory. As a result, an additional gage was attached to the tie plate edge 1 in. from the tack weld, in line with the column flange edge on all other plates. The predicted strain at the edge gage based on the applied jack load was in agreement with the measured strain. Hence, in all subsequent tests the stresses at the

tack welds were controlled by strain gages attached to the tie plate edge, 1 in. from the end of the tack weld.

Because of the inconsistencies with bending theory found above, extra strain gages were placed on several tie plates to investigate the stress distribution. The results are reported in Chapter 4. The stress range at the tack weld for the first set of tie plates was estimated from these measurements.

Initially the tie plates were tested in pairs, one bolted to each flange of the loading beam. Those tie plates marked with subscript "a" were bolted to the east side and those with subscript "b" were bolted to the west side. A problem with torsion was encountered and this twisting was minimized by adjusting the hydraulic jack's position under the beam until the deviation of stresses between the two tie plates was a minimum. For the third tie plate set, TPA-3a and TPA-3b, the W12 x 120 loading beam was split down the web to minimize the unequal distribution of force to each plate.

When one of the tie plates in the set developed a 1-1/2 in. or greater length crack, a steel strap was bolted over the plate so that the second plate test could be continued. But the crack continued to grow under the steel strap. As the crack grew in one of the tie plates, redistribution of load was observed to occur between the two plates. Therefore after TPA-3a and TPA-3b tie plates were tested the procedure was changed and the remaining tie plates were tested one at a time. The test tie plate was attached to the west side of the

setup. The east side tie plate was only bolted to the column and beam and no tack welds were placed. In addition a strain gage was placed on the bottom edge of the unwelded tie plate to monitor the load distribution between the two tie plates. All tie plates with specimen numbers lacking subscripts "a" or "b" were tested individually.

4. TEST RESULTS

4.1 Observed Stress Distribution in the Tie Plates

Because of the discrepancy between the measured strain and predicted jack load on the first test setup, several tie plates were extensively gaged to determine the stress distribution in the tie plate at the critical cross-section. Figure 6 shows the location of the strain gages used in the first study. Also shown is the predicted and measured strain distribution for a nominal plate bending stress of 10 ksi at the end of the tack weld. Tests were also run on TPC-3 and TPC-5. On TPC-5 the column bolts were only hand tightened. Figures 7 and 8 show the location of the strain gages and compares the measured and predicted strains for a stress of 10 ksi. All of the tests showed that the strains on the face of the tie plate were smaller than expected based on bending theory. Apparently the bolted connection between the tie plate and loading beam flange interacted because of the shear forces developed on the plate-beam flange faying surface. Hence there was a decrease in the estimated bending stress away from the plate edge.

4.2 Results of Tie Plate Fatigue Tests

Twenty tie plates were tested at stress ranges which varied between 7.3 and 30 ksi. Shown schematically in Appendix A are the fatigue cracks that formed in the tie plates. Because of the high residual stresses at the tack weld, a number of the tie plates

developed fatigue cracks at the tack weld on the tie plate's compression edge. These are marked with a subscript "c" after the tie plate's number. Only in one case, TPA-lac, did this crack grow through the tie plate thickness. Even in this case the tie plate failed on the tension side. A tie plate was considered to have failed when the crack reached a length of 1-1/2 in. Table 3 summarized the results for each tie plate. Those cracks which developed on the compression edge are also included in Table 1 since they would have grown much larger when subjected to the stress reversals experienced by the tie plates in the bridge.

The results of the tie plate tests are also summarized in Figure 9. This figure shows the stress range as a function of cycle life. The test data are compared with the AASHTO Category D^4 which provides a reasonable estimate of the lower bound fatigue strength of this detail.

In addition to the fatigue failures which originated at the tack weld, the unwelded plate used on the east side of the test setup for the individual testing of the tie plates developed an 8-1/8 in. fatigue crack. This fatigue failure is discussed in Appendix B.

5. EVALUATION OF STRESS CONCENTRATION CONDITION AT TACK WELD TOE

In order to evaluate crack growth in the tie plate, the stress concentration at the tack weld termination was needed[2,3]. A finite element analysis of the plate using the three dimensional solid element (eight node brick) of the SAP IV[5] finite element program was performed to estimate the stress concentration factor. The model used for the analysis consisted of the tie plate and bracket flange in the immediate vicinity of the bolted connection between these two members as shown schematically in Fig. 10.

The bracket flange and tie plate are connected by two 2 in. long tack welds and eight bolts. In the finite element model the tack weld was represented by a 2 in. long triangular wedge attached to the edge of the tie plate and the face of the flange. The adjacent faces of the tie plate and flange were unattached except at the bolt locations. Here the two faces shared four nodes, one at each corner of a one inch square centered on the bolt hole center line. Though this is not the same as the bolted joint, it does provide a relatively stiff joint as do the bolts, torqued to one-half of the required torqued, under the low shear stresses experienced by the tie plate. In addition the bolts are far enough away from the point of interest, the tack weld termination, that any errors introduced by the modeling of the bolts will not significantly effect the results of the finite element analysis.

Appropriate forces from the bending moment and shear were applied to the right-hand end of the bracket flange and the left-hand end of the tie plate. The resulting stresses in the region where the stress distribution was investigated agreed with bending theory and therefore not with the measured stresses. This could be expected since the bolt clamping force was not modeled and therefore the faying surface interaction was not included, except at the common node points.

Using the nodal displacements from this analysis as boundary conditions; a second much finer mesh analysis of the region in the immediate vicinity of the tack weld termination was performed. The element stresses at the base of the tack weld termination obtained from the analysis were then utilized in a least square fit using a complete second order polynominal to approximate the stress concentration at the weld termination.

The above analysis was performed for the extreme case of the tack weld having a vertical termination and also for the case of the tack weld termination having a slope of 1 to 3.75, which was typical for the tie plate specimens. For the vertical tack weld termination the stress concentration factor was estimated to be 2.82, whereas the sloping tack weld termination provided a value of 2.80. As can be seen the slope has little effect on the stress concentration, therefore in all calculations involving the stress concentration factor a value of 2.80 was used.

6. FRACTURE MECHANICS ANALYSIS OF CRACK GROWTH IN THE TIE PLATES

An analytical study of the crack growth in tie plates was undertaken to assist in evauating the experimental results. The differential equation of crack growth proposed by Paris[11] was used for this analysis. This equation states

$$\frac{da}{dN} = C\ (\Delta K)^n \tag{1}$$

where $\frac{da}{dN}$ is the rate of crack propagation, ΔK is the stress intensity range, and C and n are material constants. C and n were assumed to be constant over the full range of ΔK and were taken to be 2×10^{-10} and 3 respectively. These are rounded values of those found by Hirt and Fisher[12] and used in Ref. 3 to evaluate crack growth at stiffener and attachment details. The stress intensity range is dependent on a number of variables and therefore must be evaluated for each configuration encountered.

The number of cycles to failure (N) can be obtained by integrating Eq. 1 from the initial crack size (a_i) to the final crack size (a_f). The result of this integration is:

$$N = \frac{1}{C} \int_{a_i}^{a_f} \frac{1}{(\Delta K)^n}\, da \tag{2}$$

In order to perform the integration an estimate of the initial crack size is needed. The range of initial weld flaw sizes at

the toe of fillet welds was reported to vary from a low of 0.00075 in. to a maximum of 0.02 in., with an average of 0.003 in.[8,9]. Reasonable agreement with these observations was provided in subsequent studies at Lehigh University[2,10]. Flaws from tack welds would in all probability have larger sizes. Therefore the initial crack size used in the analysis was varied from 0.001 to 0.003 in. A crack length of 1.5 in. was used to define failure of the tie plate.

For each initial crack size used in the integration of Eq. 2, a threshold stress range was also calculated. The threshold stress intensity range of 3.3 ksi $\sqrt{\text{in.}}$ found by Klingerman[11] along with the assumed initial crack size was substituted into the stress intensity function to obtain the threshold stress range.

Two models were used to estimate ΔK in the analytical investigation of the tie plate crack propagation. Each involved the use of a decay function for the stress concentration at the tack weld termination.

In both models it was assumed that the initial crack was a corner crack, since the tie plate cracks were observed to start as corner cracks from visual inspection of the crack surface. This corner crack can be seen in the photograph of the plate TPC-2b's crack surface shown in Fig. 11.

The first model consisted of a three stage integration of Eq. 2 shown schematically in Fig. 12. For the first stage the stress intensity factor (K) was defined as

$$K = K_T\left(\frac{a}{t}\right)\ \sigma\sqrt{\pi a} \tag{3}$$

where σ is the stress, a is the crack size and $K_T\left(\frac{a}{t}\right)$ is the stress concentration decay function[3]. The decay function was taken as

$$K_T\left(\frac{a}{t}\right) = K_T - 2\left(K_T - 1\right)\frac{a}{w} + \left(K_T - 1\right)\left(\frac{a}{w}\right)^2 \tag{4}$$

where K_T is the stress concentration factor and w is the weld size[3]. Since this decay function was derived for a different detail, w had to be modified. The stress concentration effect was taken into account until a crack length of 0.26 in. was obtained. This corresponded to $\sqrt{2}$ times the weld size at the end of the weld toe as shown in Fig. 12 Equation 2 was integrated from the initial crack sizes of 0.001, 0.003, 0.02, and 0.03 in. to the final crack size of 0.26 in. considering the stress concentration factor to be 2.80 as derived from the finite element analysis.

For the second crack growth stage, Eq. 2 was integrated from 0.26 in. to the plate thickness (t) of 0.5 in. The stress intensity function used the secant correction for a free surface and therefore was defined as[3]

$$K = \sigma\sqrt{\pi a}\ \sqrt{\sec\frac{\pi a}{2t}} \tag{5}$$

The shaded region shown in Fig. 12 was not included in the analysis, as the number of cycles required to propagate the crack though this region was small.

During the first two stages of growth, the crack was not appreciably affected by the moment gradient in the tie plate. But in the third stage, the crack was growing in a region of moment gradient and therefore the following stress intensity factor[12] was used:

$$K = \sqrt{\frac{2\omega}{\pi a} \tan \frac{\pi a}{2\omega}} \quad x \quad \frac{0.923 + 0.199 \quad 1 - \sin \frac{\pi a}{2\omega}}{\cos \frac{\pi a}{2\omega}} \qquad (6)$$

where ω is the plate width. Equation 2 was then integrated from a crack size of 0.5 in. to 1.5 in.

In addition to varying the initial crack size, the stress concentration factor of 2.80 was varied by ±10%, i.e. 2.52 to 3.08. This was done to evaluate the effect of a deviation of the stress concentration factor from the value derived from the finite element analysis.

The results of the first analytical model used in the analysis of crack propagation in the tie plate are shown in Fig. 13 for the three initial crack sizes, 0.001, 0.003, 0.02 and 0.03 in., and a stress concentration factor of 2.80. Also shown are the threshold stress range for each initial crack. Design Category D and the test data are plotted in Fig. 13 for comparison. It can be seen that the lower life estimate for this model is just above Category D, with all but three of the test data points between the outer two prediction lines. Two of these points fall just below the lower life estimate and suggest a slightly larger initial crack size than assumed. The third point,

at 30 ksi, is tie plate TPC-1b. The stress range was estimated for this tie plate. In addition the crack was only 3/4 in. long when the test was stopped. Integrating the third stage of growth from 3/4 in. to 1-1/2 in. at a 30 ksi stress range, adds 20,000 cycles to its life and provides better agreement with the lower bound life estimate. By comparing Fig. 13 with Figs. 14 and 15, the results of using stress concentration factors of 2.52 and 3.08 respectively in the first analytical model, it can be seen that variations in the stress concentration factor has little effect on the predicted life. The first analytical model provides a threshold stress range of 4 ksi based on an initial crack size of 0.03 in. and stress concentration of 3.08 and a reasonable lower bound estimate of the tie plate's fatigue life.

In the second analytical model, stages I and II were combined. For this combined stage the stress intensity factor was expressed as

$$K = K_T \left(\frac{a}{t}\right) \sigma \sqrt{\pi a} \sqrt{\sec \frac{\pi a}{2t}} \tag{7}$$

where

$$K_T\left(\frac{a}{t}\right) = K_T \left[1 - 3.215 \frac{a}{t} + 7.897\left(\frac{a}{t}\right)^2 - 9.288\left(\frac{a}{t}\right)^3 + 4.086\left(\frac{a}{t}\right)^4 \right] \tag{8}$$

is the decay function with $a \leq t$, the plate thickness[3]. With this formulation of the stress intensity, Eq. 2 was integrated from the initial crack sizes of 0.001, 0.003 and 0.03 in. to a crack size of

0.5 in. The second stage of crack growth was identical to the third stage of growth used for the first model.

The results of using model II are summarized in Figs. 16, 17 and 18 along with Category D and the test data. Figure 16 is for the stress concentration factor equal to 2.80. As can be seen in this figure the lower bound estimate of the stress range-cycle life relationship is closer to Category D than the first model and all test data falls between the lower and upper bound estimates of life. Figures 17 and 18 are the results obtained using a stress concentration of 2.52 and 3.08 respectively. Changing the stress concentration factor had little effect on the predicted life. About the same crack growth threshold stress range (4 ksi) was predicted for an initial crack size of 0.03 in. and stress concentration factor of 3.08.

Figures 13 through 18 demonstrate that Category D is a reasonable lower bound life estimate for the tie plate with tack welds. Only an extreme condition would cause the crack growth threshold to fall below the fatigue limit for Category D. It also can be seen that all the test data fall above Category D.

7. SUMMARY AND CONCLUSIONS

The following summary and conclusions are from the laboratory tie plate tests and the analytical studies of the tie plates.

1. The stresses on the face of the tie plate at the critical section were smaller than expected based on bending theory. The stresses on the plate edge did conform to bending theory. Apparently the bolted connection between the tie plate and loading beam interacted because of shear forces developed on the plate-beam flange faying surface. Hence there was a decrease in the estimated bending stresses away from the tie plate edge. This decrease had no influence on crack growth from the tack weld on the tie plate edge.

2. The fatigue cracks originated at the toe of the tack weld termination, at the corner where the tie plate edge and face meet. From here the crack grew through the thickness and up the face of the tie plate.

3. A finite element analysis of the stress concentrations at the tack weld termination revealed that the stress concentration was not sensitive to variations in the slope of the weld termination. A stress concentration factor equal to 2.80 was found for the typical slope on the test specimens.

4. Two different analytical models, using different decay functions for the stress concentration, were used in the fracture mechanics analysis of crack growth in the tie plates. Even with a ±10% variation of the stress concentration factor both models provided a reasonable lower bound estimate of the tie plate fatigue life; with failure defined as a 1-1/2 in. or longer fatigue crack.

5. With failure of a tie plate defined as a fatigue crack of 1-1/2 in. or more, Category D of the AASHTO specifications provides a reasonable lower bound for the fatigue life data obtained from the twenty tie plates tested and is in agreement with the lower bounds found from the two analytical models use. Therefore Category D can be used to define the fatigue strength of these tie plates.

TABLE 1 SUMMARY OF TIE PLATE DATA

Tie Plate	S Ranage (ksi)	S Minimum (ksi)	N Failure
TPA-1a	13.8	2.0	1,281,800
-1ac	18.2	2.3	1,281,800
-1b	15.6	2.1	1,018,500
TPA-2a	12.3	2.0	3,363,200
-2b	11.8	2.0	3,363,200
TPA-3a	7.8	1.9	7,466,700
-3b	8.2	2.3	26,354,200*
TPA-4	20.0	2.0	452,000
-4c	21.4	2.0	481,500
TPA-5	20.0	2.0	552,000
-5c	20.2	2.4	600,000
TPA-6	10.0	2.0	3,366,400
-6c	9.9	2.0	3,670,500
TPA-7	10.0	2.0	4.947,000
TPC-1a	30.0	3.8	71,800**
-1b	30.0	3.8	71,800
TPC-2a	13.4	1.6	1,046,600
-2b	12.3	1.5	15,936,700
TPC-3	8.0	2.0	20,522,400*
-3c	7.3	1.9	12,619,700
TPC-5	16.0	2.0	3,314,600
-5c	11.7	1.9	2,283,700
TPC-6	16.0	2.0	628,500
-6c	16.8	2.3	628,500
TPC-7	24.0	2.0	211,000
TPC-8	24.0	2.0	252,000

* No detectable crack

** Test stopped before failure, see crack documentation

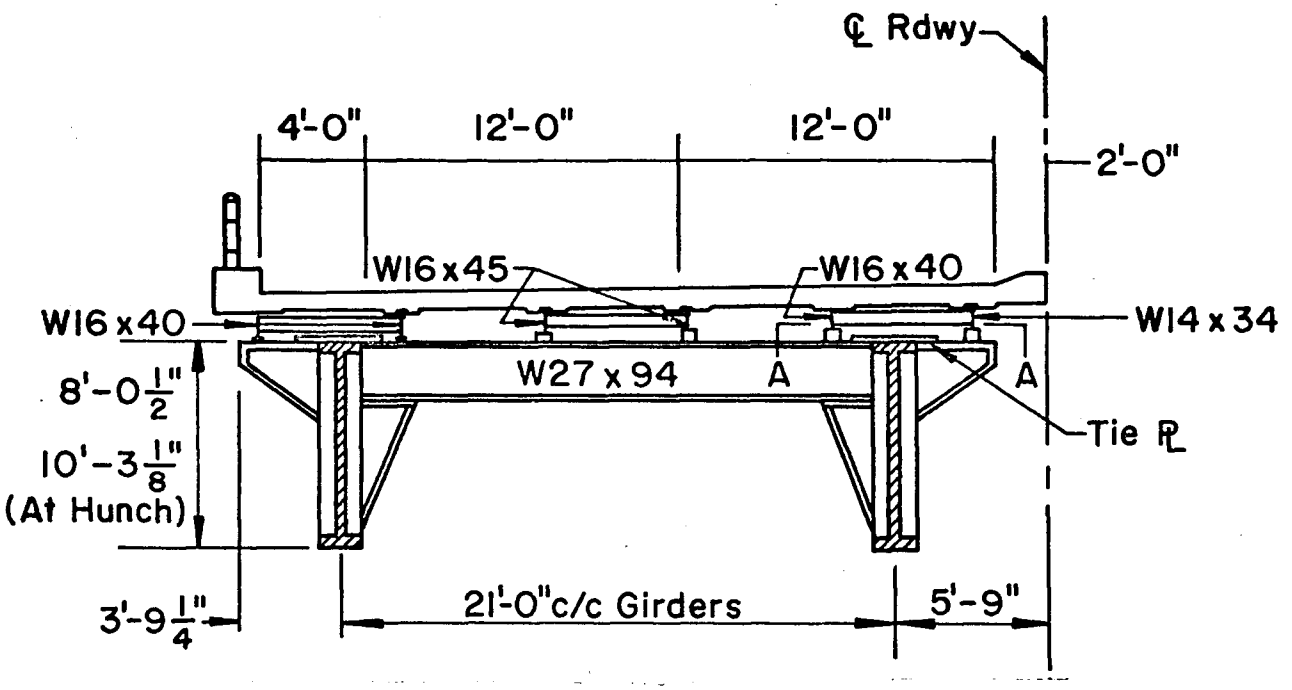

Fig. 1a Cross-Section at Lehigh Canal Bridge

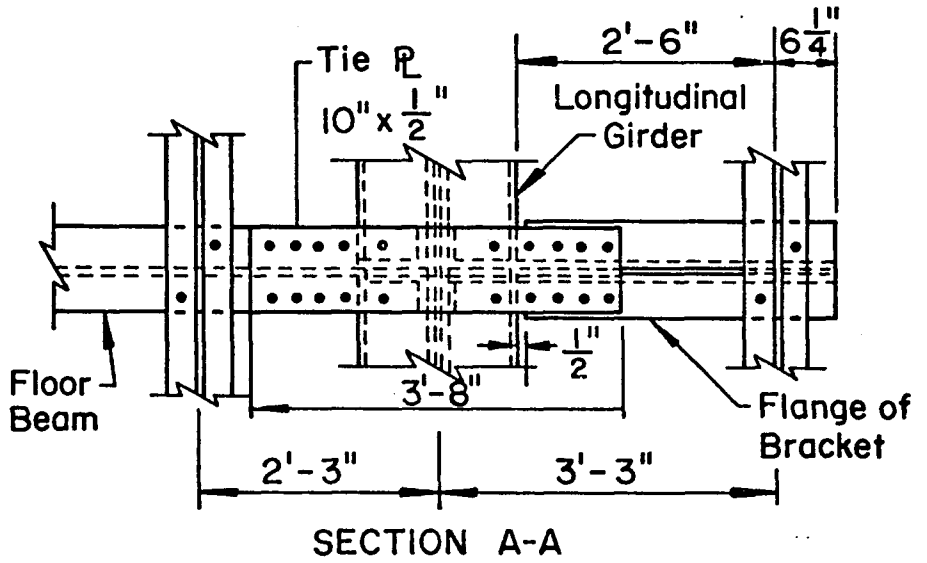

Fig. 1b Tie Plate Detail at Floor Beam Bracket

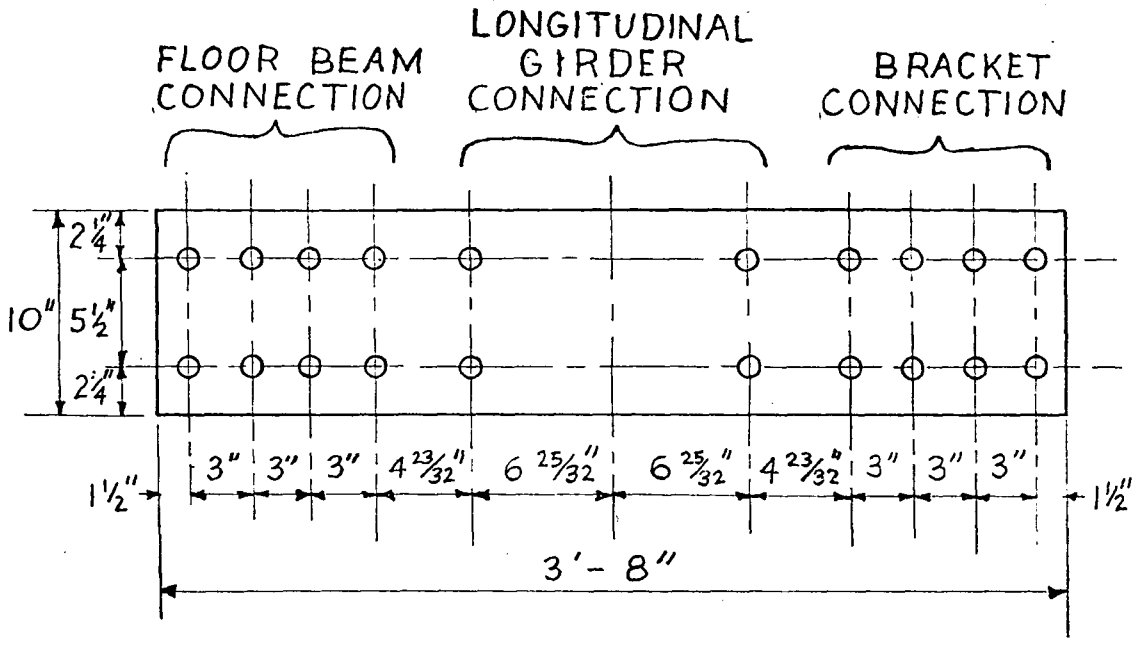

NOTES
1. ALL HOLES 15/16" ϕ
2. PLATE ½" THICK

Fig. 2 Typical Lehigh Canal Bridge Tie Plate

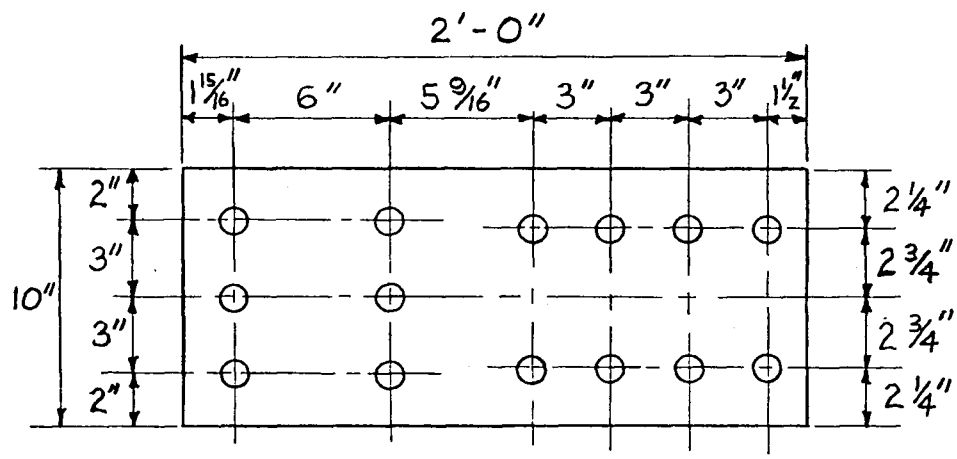

NOTES
1. ALL HOLES 1⅛" ϕ
2. ALL EDGES SAW CUT
3. PLATE ½" THICK

Fig. 3 Test Specimen

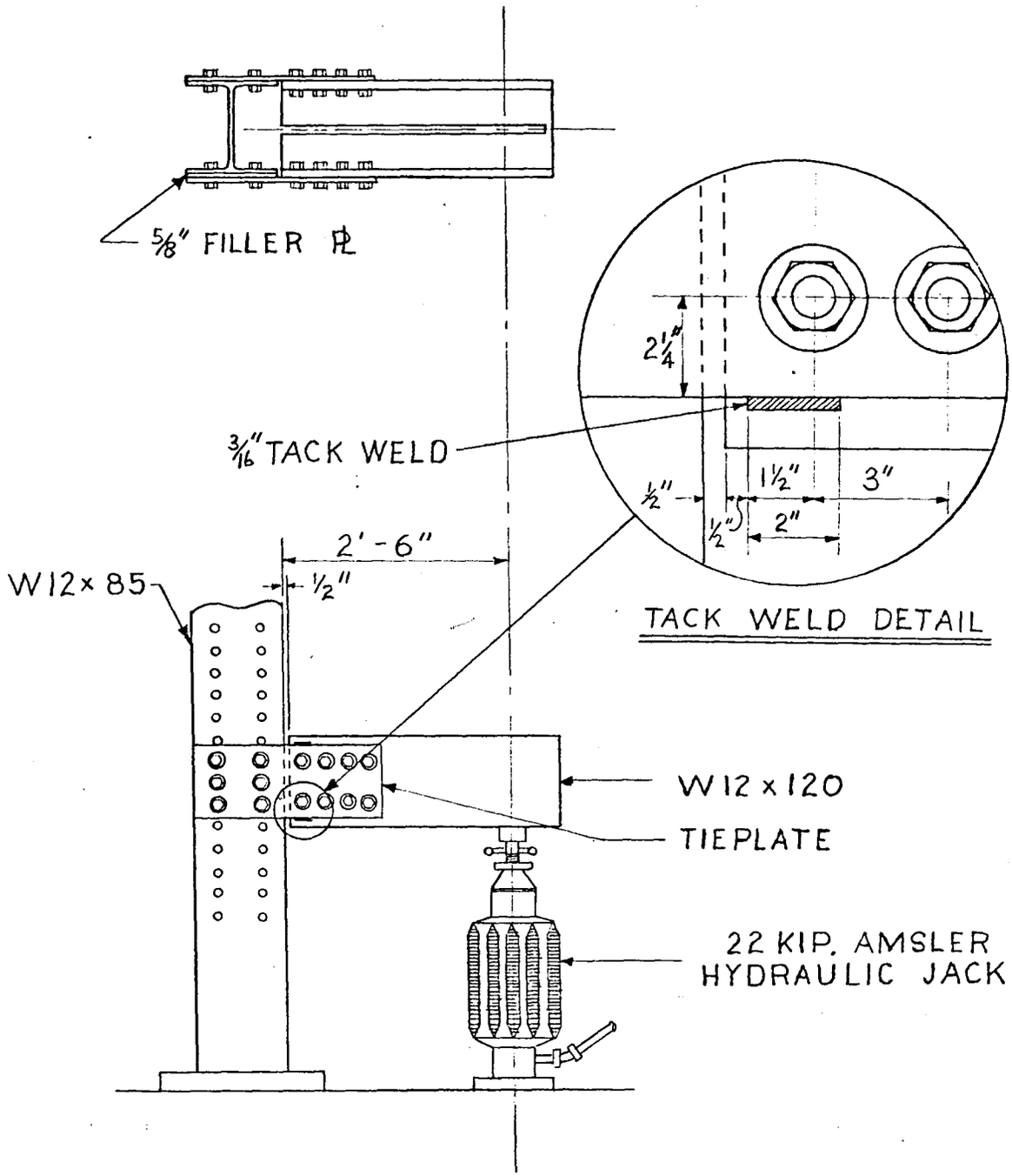

Fig. 4 Tie Plate Test Setup

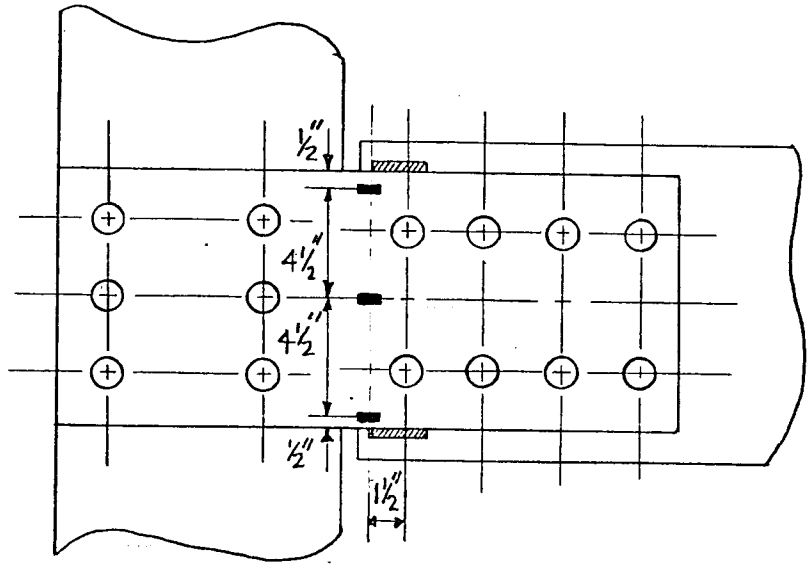

Fig. 5 Strain Gages on TPC-1a and TPC-1b

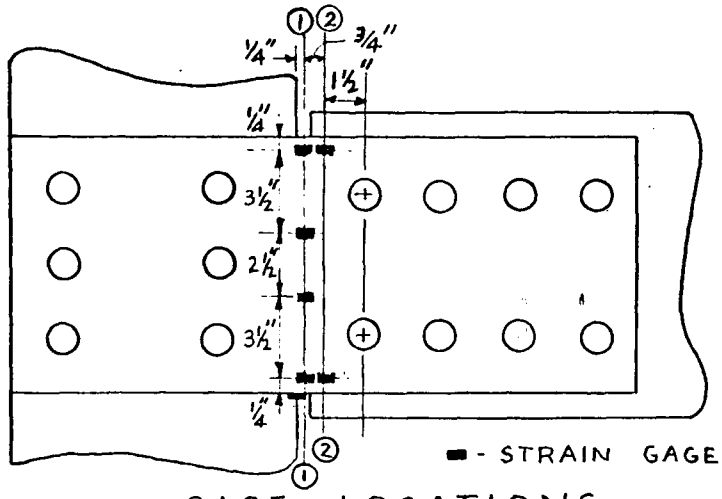

GAGE LOCATIONS

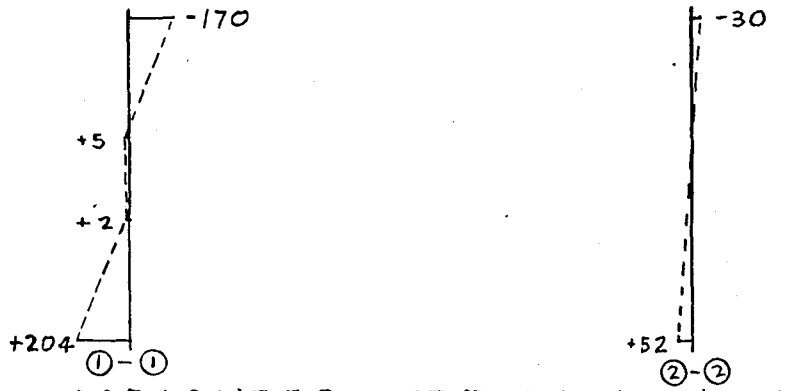

MEASURED STRAIN (μ-IN/IN)

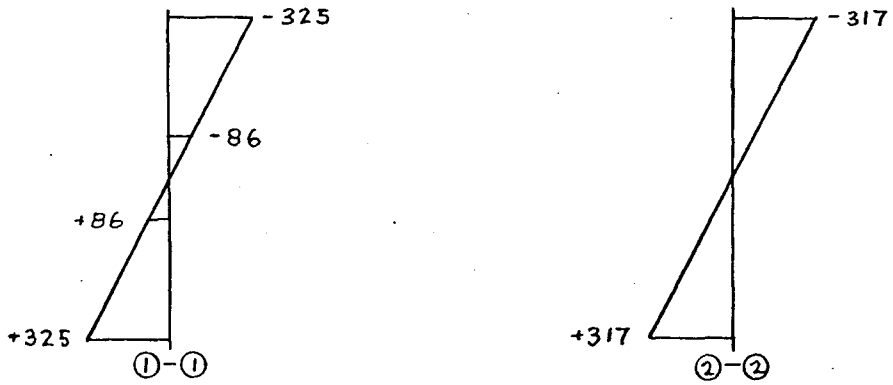

COMPUTED STRAIN (μ-IN/IN)

Fig. 6 Strain Measurements of First Stress Distribution Test

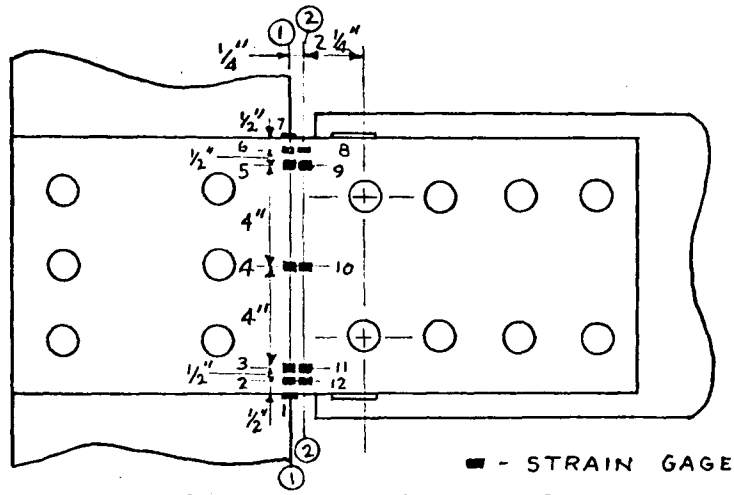

GAGE LOCATIONS

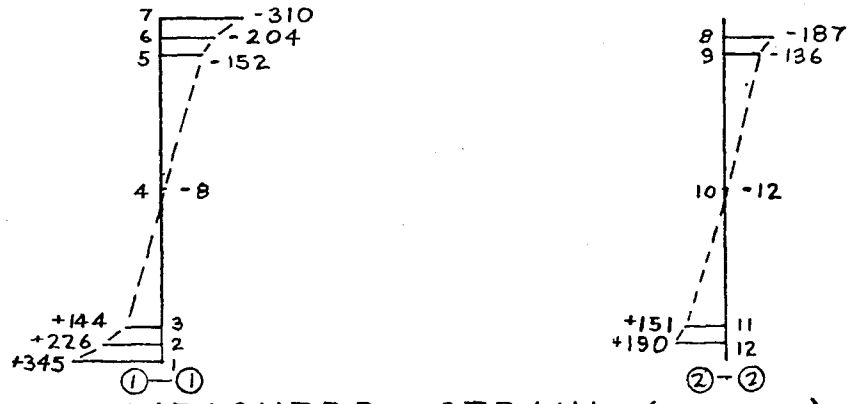

MEASURED STRAIN (μ-IN/IN)

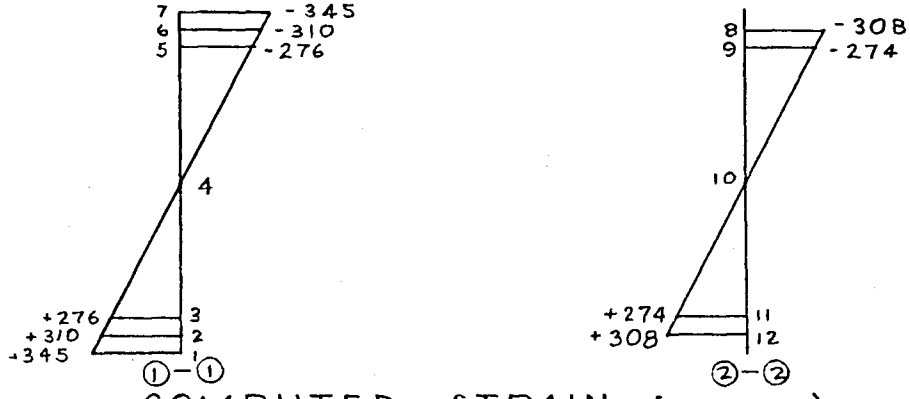

COMPUTED STRAIN (μ-IN/IN)

Fig. 7 Strain Measurements on TPC-3

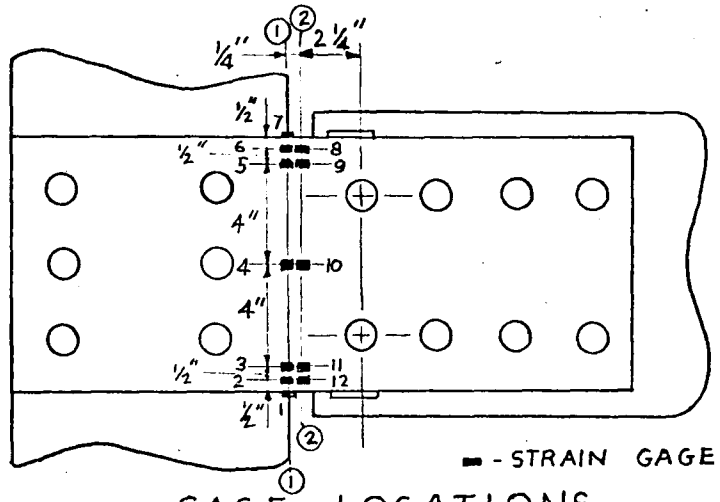

GAGE LOCATIONS

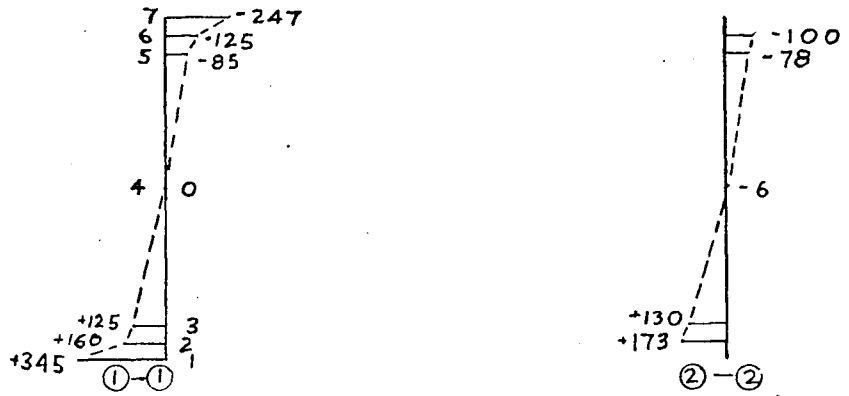

MEASURED STRAIN (μ-IN/IN)

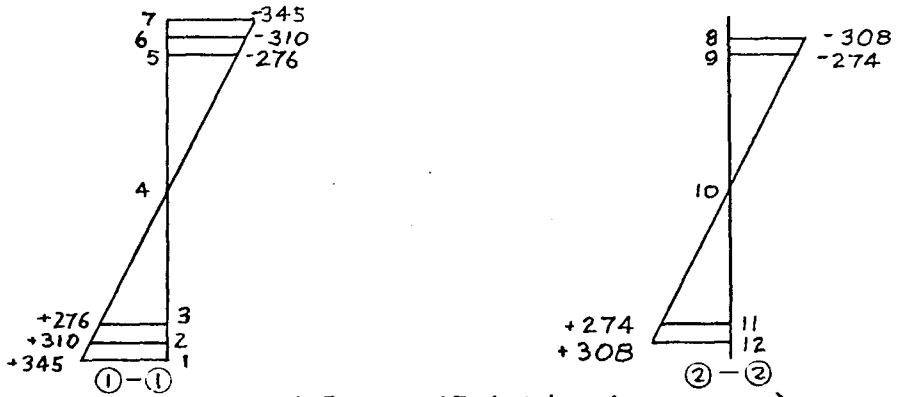

COMPUTED STRAIN (μ-IN/IN)

Fig. 8 Strain Measurements on TPC-5

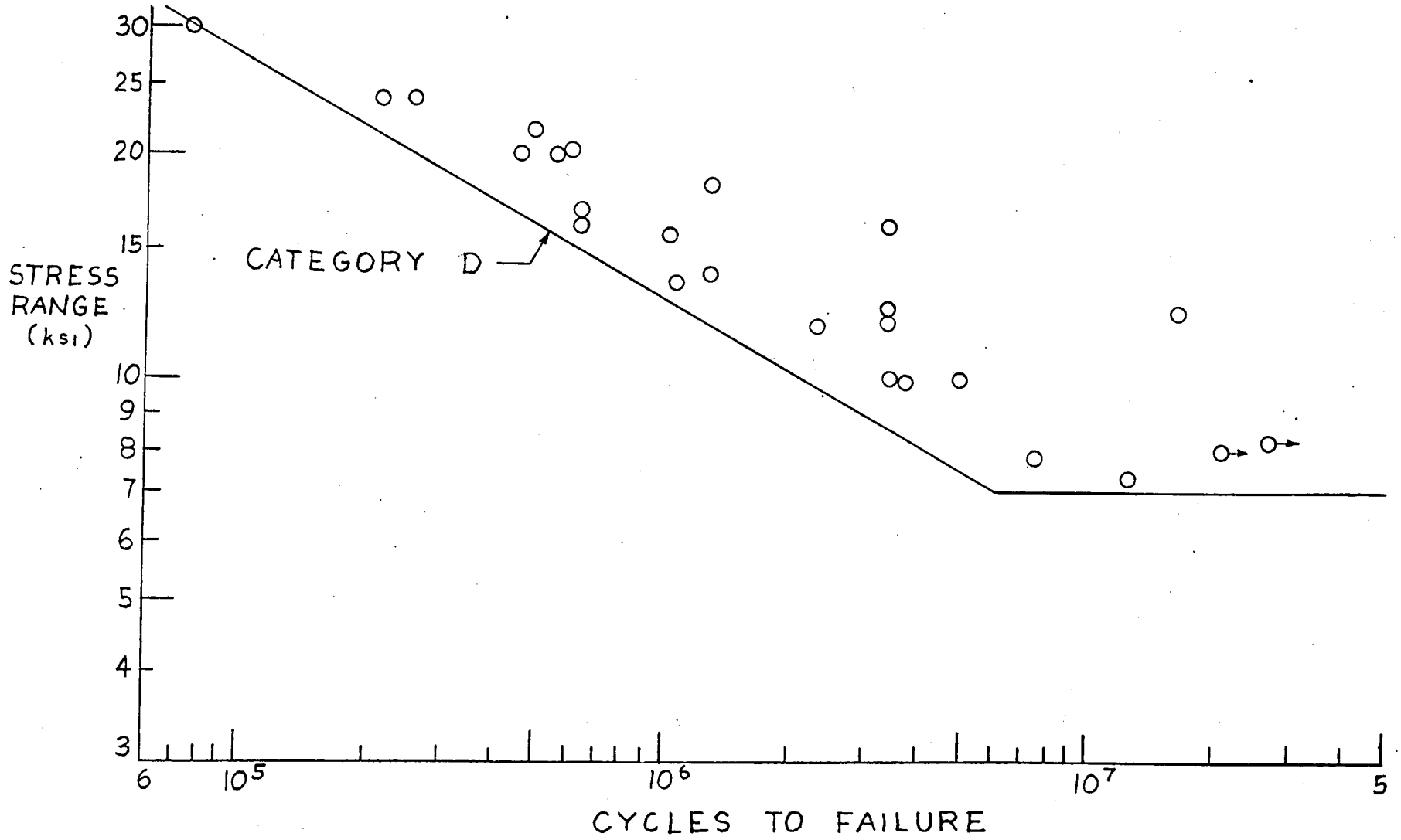

Fig. 9 Summary of Test Results

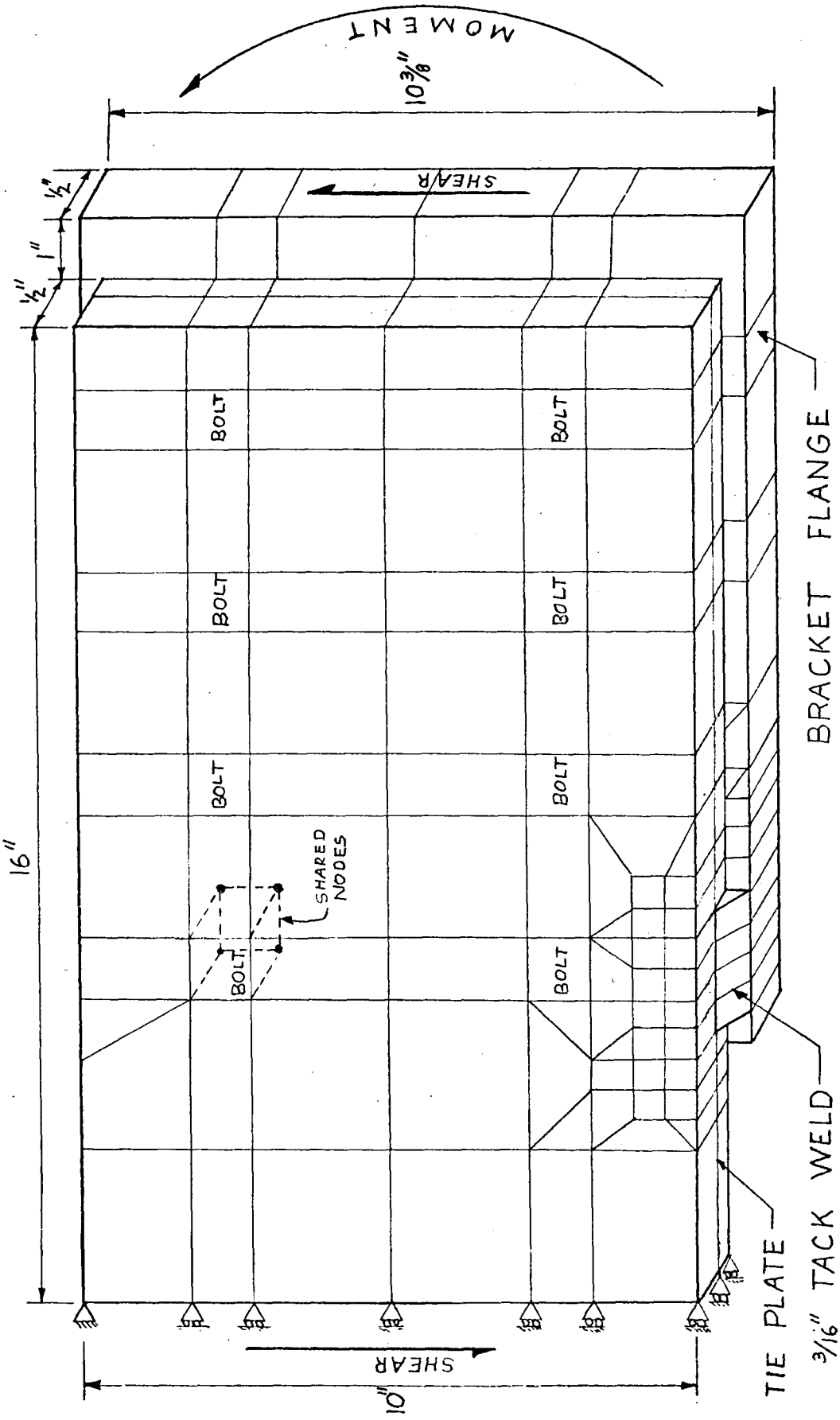

Fig. 10 Schematic of Finite Element Model

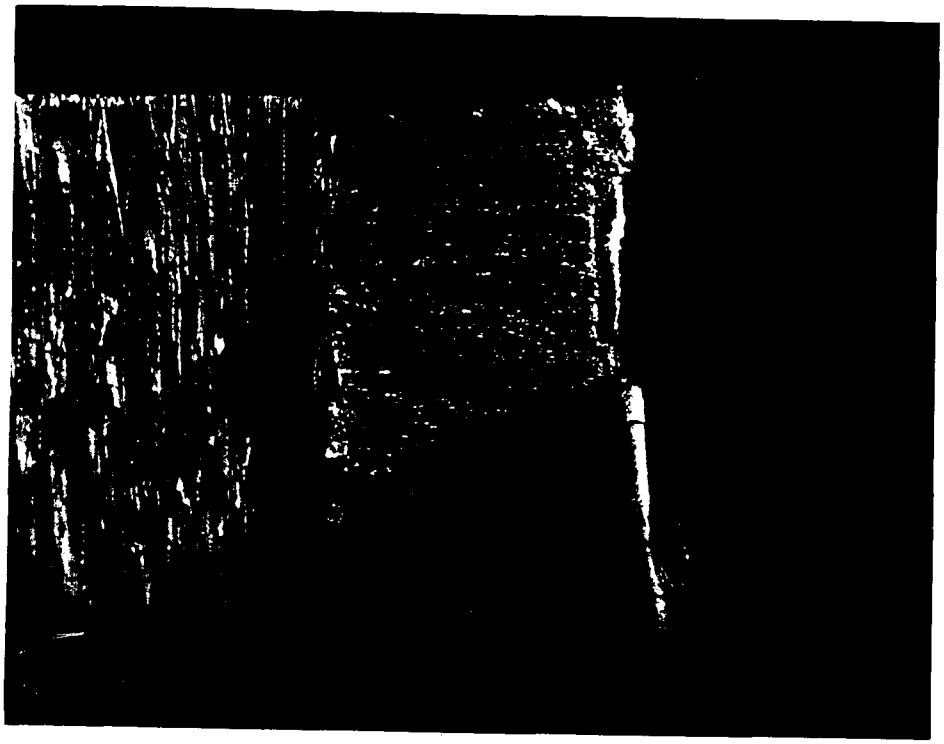

Fig. 11 Corner Crack in Tie Plate TPC-2b

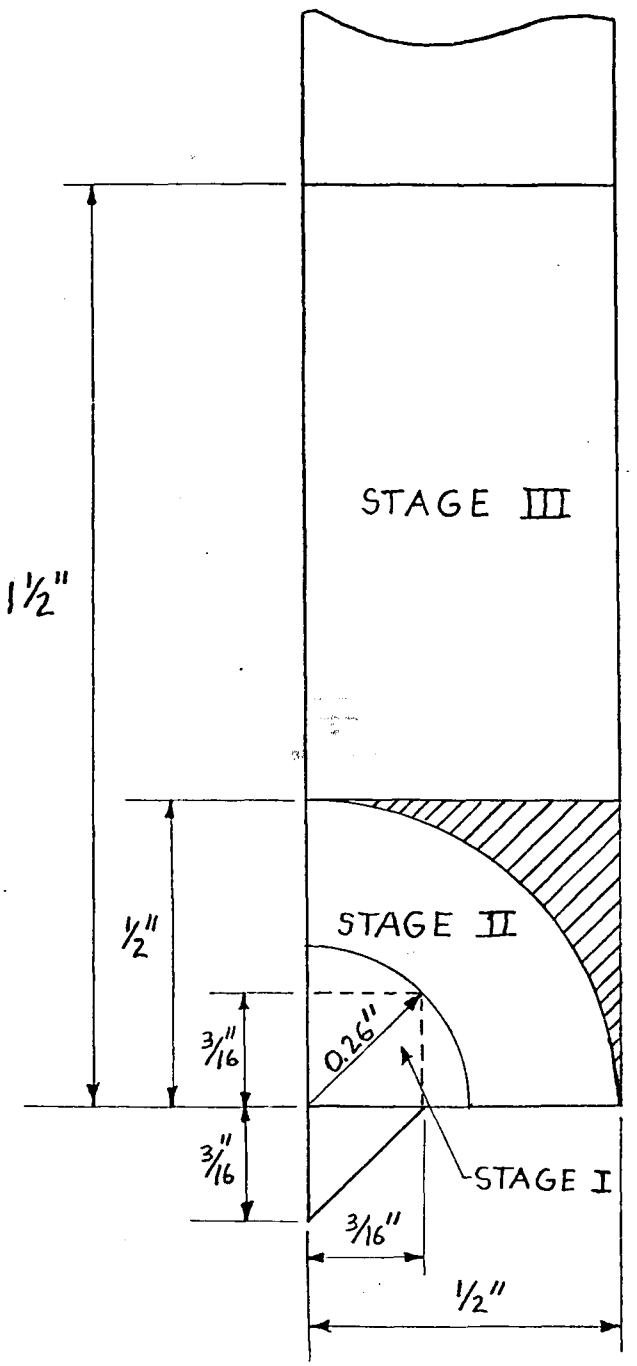

Fig. 12 Schematic of First Analytical Model's Three Stage Integration

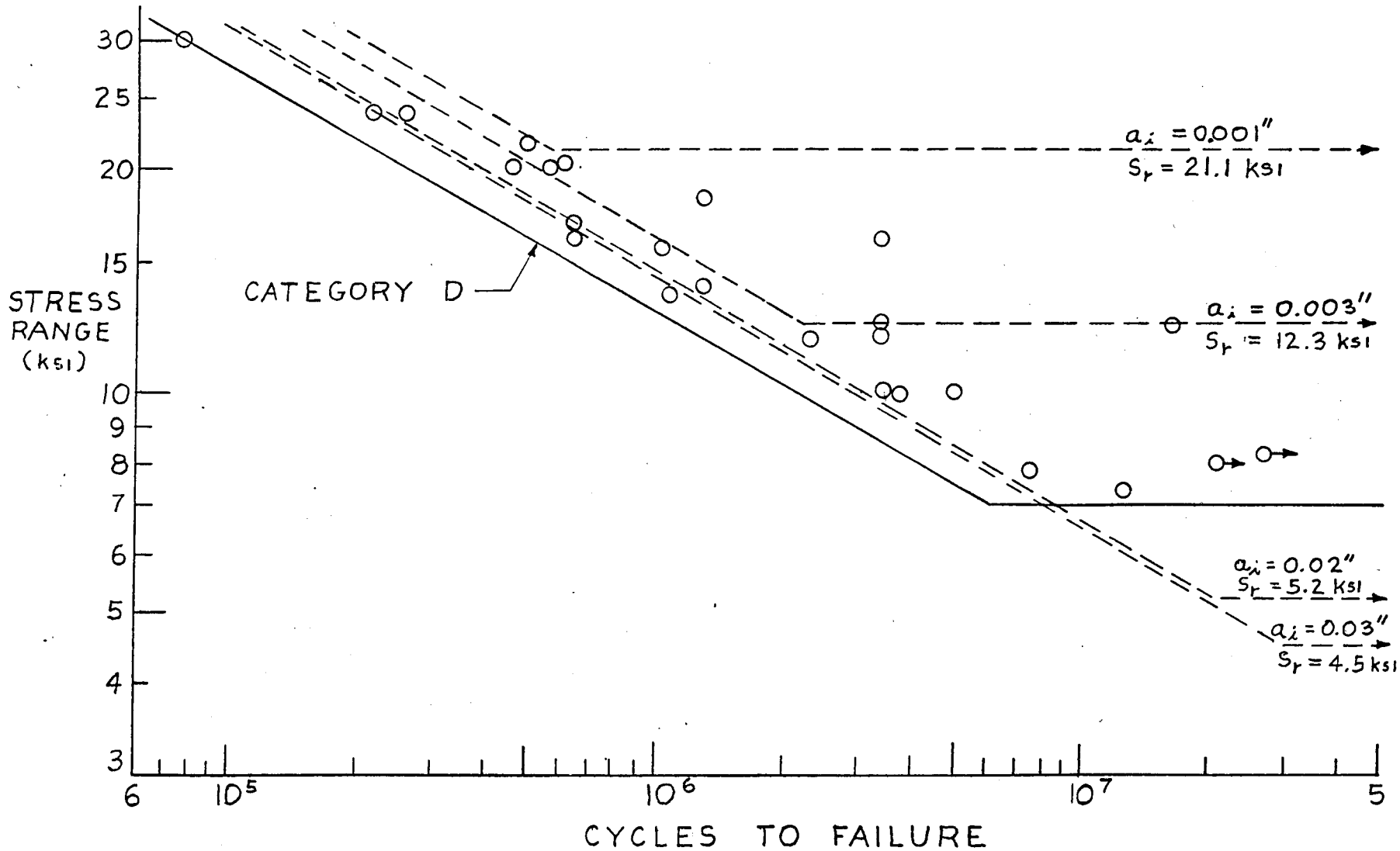

Fig. 13 Comparison of First Analytical Model to Test Results - K = 2.80

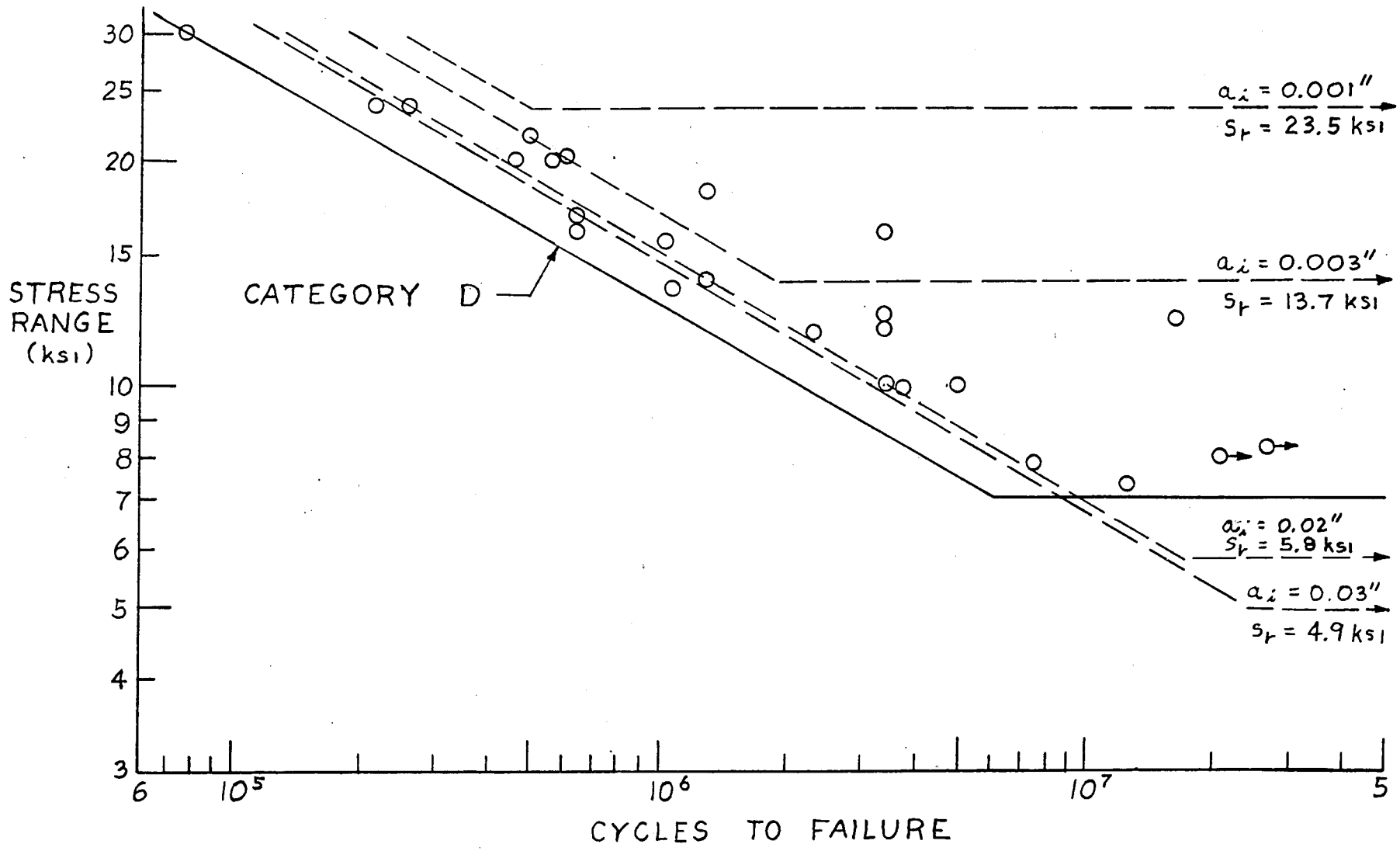

Fig. 14 Comparison of First Analytical Model to Test Results - K = 2.52

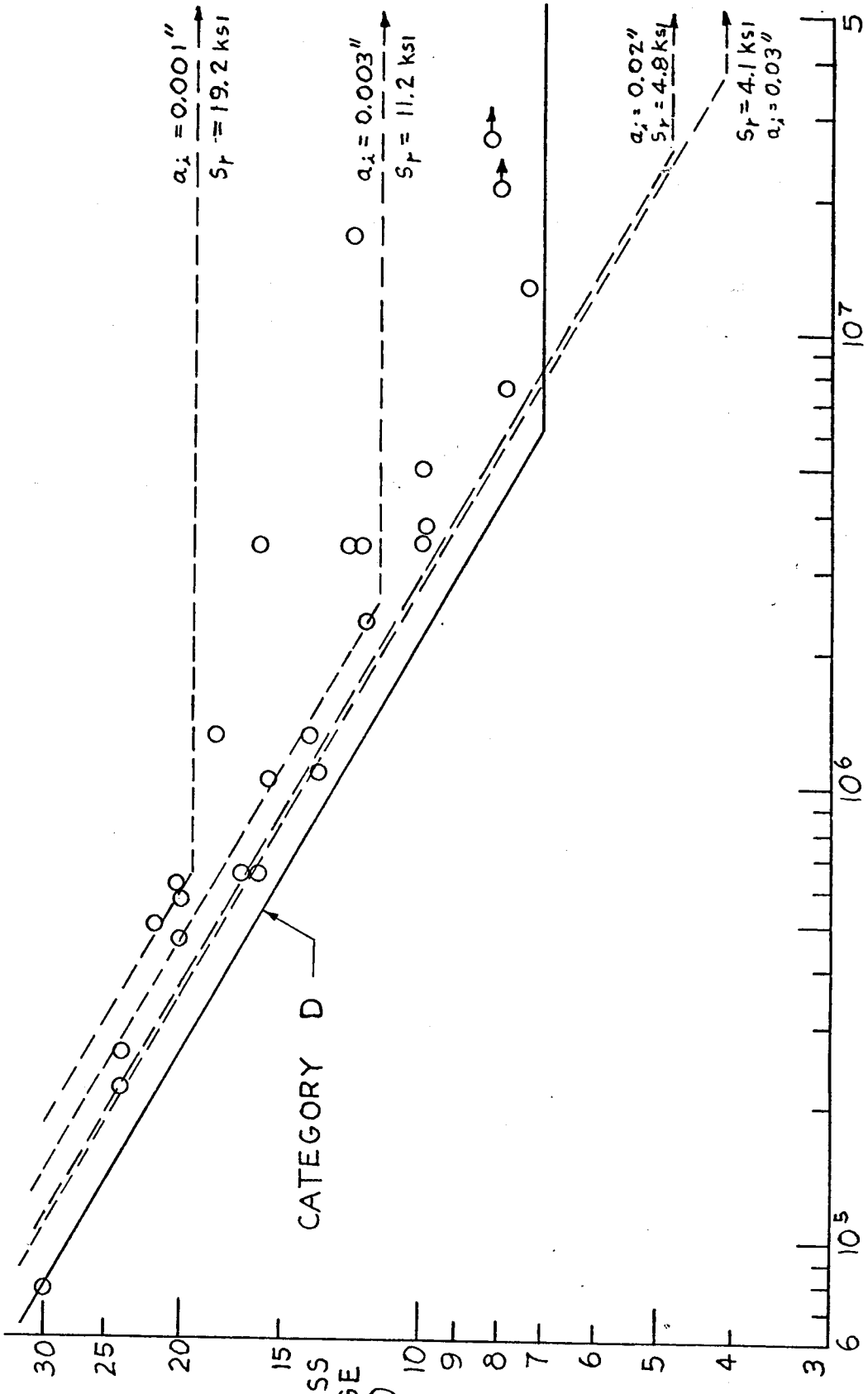

Fig. 15 Comparison of First Analytical Model to Test Results - K = 3.08

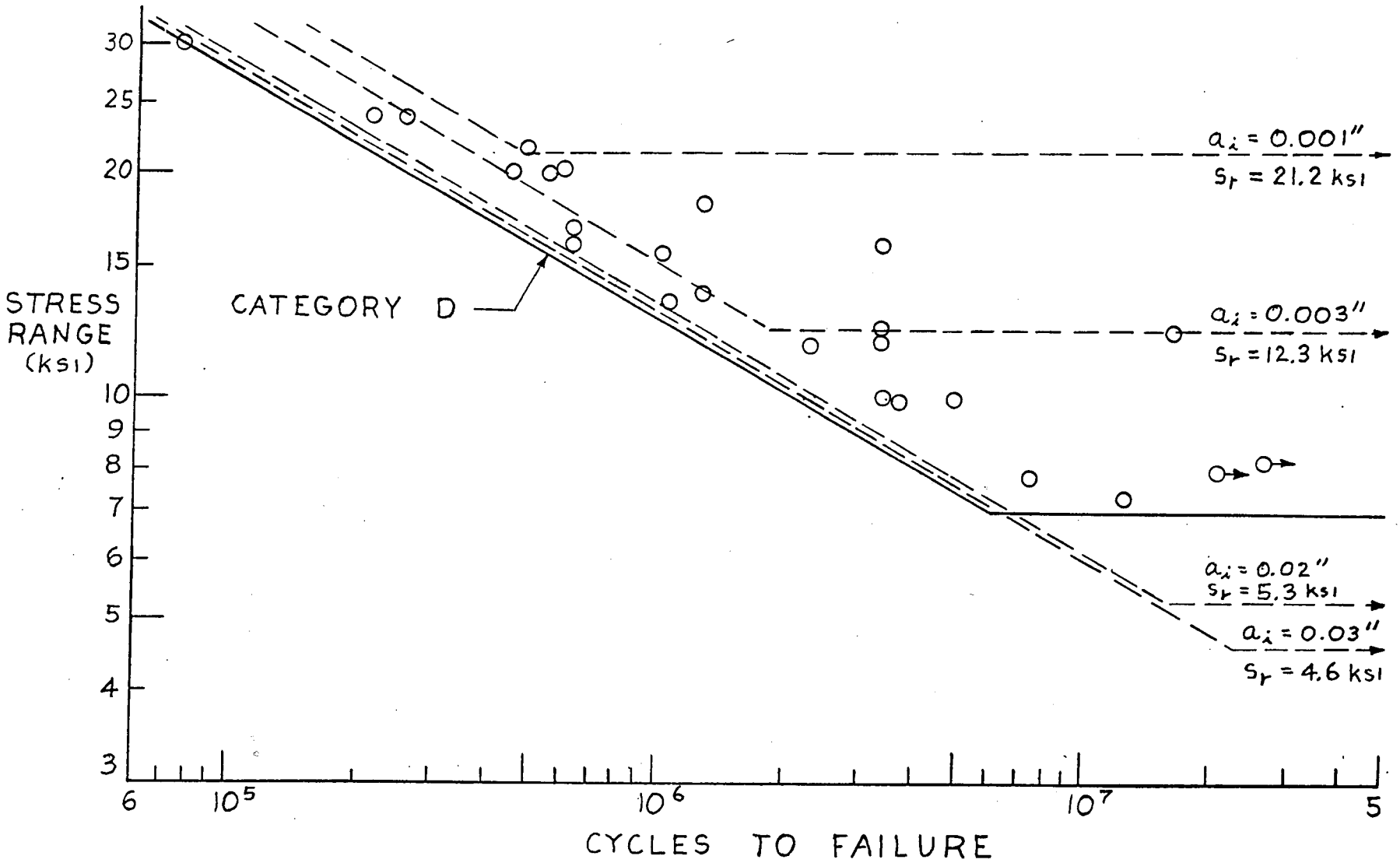

Fig. 16 Comparison of Second Analytical Model to Test Results - K = 2.80

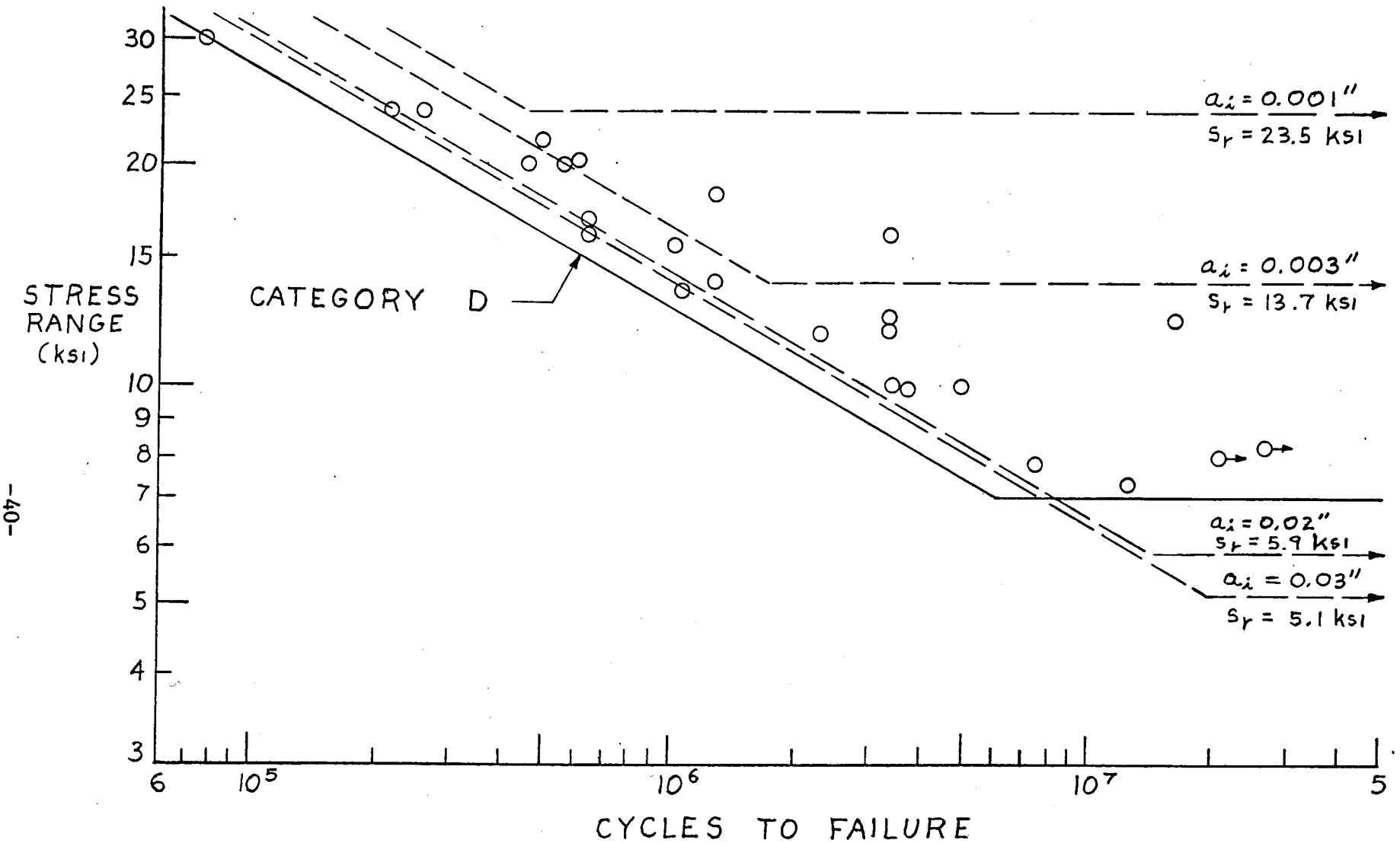

Fig. 17 Comparison of Second Analytical Model to Test Results - K = 2.52

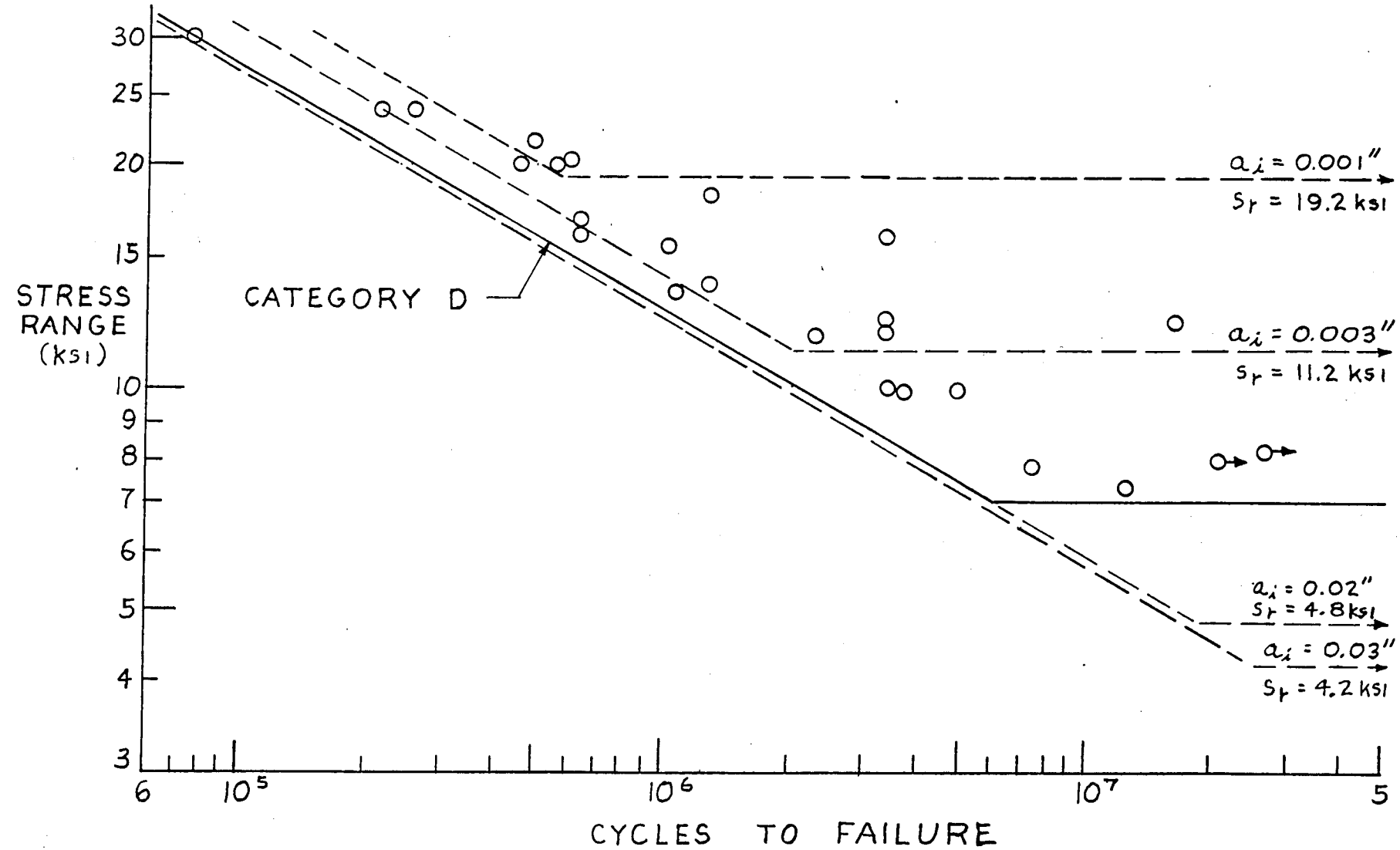

Fig. 18 Comparison of Second Analytical Model to Test Results - K = 3.08

REFERENCES

1. Fisher, J. W., Yen, B. T. and Marchica, N. V.
   FATIGUE DAMAGE IN THE LEHIGH CANAL BRIDGE, Fritz Engineering Laboratory Report No. 386.1, Lehigh University, November 1974.

2. Fisher, J. W., Albrecht, P. A., Yen, B. T., Klingerman, D. J. and McNamee, B. M.
   FATIGUE STRENGTH OF STEEL BEAMS WITH WELDED STIFFENERS AND ATTACHMENTS, NCHRP Report No. 147, Transportation Research Board, National Research Council, Washington, D.C., 1974.

3. Albrecht, P. and Fisher, J. W.
   AN ENGINEERING ANALYSIS OF CRACK GROWTH AT TRANSVERSE STIFFENERS, International Association for Bridge and Structural Engineering, Zürich, Switzerland, 1975

4. American Association of State Highway Transportation Officials
   INTERIM SPECIFICATIONS BRIDGES, 1974.

5. Bathe, K., Wilson, E. L. and Peterson, F. E.
   SAPIV: A STRUCTURAL ANALYSIS PROGRAM FOR STATIC AND DYNAMIC RESPONSE OF LINEAR SYSTEMS, University of California at Berkeley, April 1974.

6. Paris, P. D., Gomez, M. P., and Anderson, W. E.
   A RATIONAL ANALYTICAL THEORY OF FATIGUE, The Trend in Engineering, University of Washington, Vol. 13, No. 1, January 1961.

7. Hirt, M. A. and Fisher, J. W.
   FATIGUE CRACK GROWTH IN WELDED BEAMS, Engineering Fracture Mechanics, Vol. 5, pp. 415-429, 1973.

8. Signes, E. G., Baker, R. G., Harrison, J. D. and Burdekin, F. M.
   FACTORS AFFECTING THE FATIGUE STRENGTH OF WELDED HIGH STRENGTH STEELS, British Welding Journal, pp. 108-116, February 1967.

9. Watkinson, F., Bodger, P. H. and Harrison, J. D.
THE FATIGUE STRENGTH OF WELDED JOINTS IN HIGH STRENGTH STEELS AND METHODS FOR ITS IMPROVEMENT, Proceedings, Fatigue of Welded Structures Conference, The Welding Institute, Brighton, England, July 1970.

10. Fisher, J. W., Sullivan, M. D. and Pense, A. W.
IMPROVING FATIGUE STRENGTH AND REPAIRING FATIGUE DAMAGE, Fritz Engineering Laboratory Report No. 385.3, Lehigh University, December 1974.

11. Klingerman, D. J. and Fisher, J. W.
THRESHOLD CRACK GROWTH IN A36 STEEL, Fritz Engineering Laboratory Report No. 386.2, Lehigh University, September 1973.

12. Tada, H. and Irwin, G. R.
K-VALUE ANALYSIS FOR CRACKS IN BRIDGE STRUCTURES, Fritz Engineering Laboratory Report No. 399.1, Lehigh University, (in preparation).

13. Polmear, I. J., Tuisk, U. U., Stephens, P. J. and Voruerg, P. R. B.
FATIGUE CHARACTERISTICS OF A SIMPLE BOLTED JOINT, The Civil Engineering Transactions of the Institute of Engineers, Australia, October 1970.

14. Fisher, J. W. and Struik, J. H. A.
GUIDE TO DESIGN CRITERIA FOR BOLTED AND RIVETED JOINTS, Wiley Interscience, 1974.

15. Kanazawa, T. and Kobayaski, A. S.
SIGNIFICANCE OF DEFECTS IN WELDED STRUCTURES, Proceedings of the Japan - United States Seminar, Tokyo, Japan, 1973.

16. Swanson, S. R.
RAMDOM LOAD FATIGUE TESTING: A STATE OF THE ART SURVEY, ASTM, Materials Research and Standards, Vol. 8, No. 4, April 1968.

17. Barsom, J. M.
FATIGUE CRACK GROWTH UNDER VARIABLE AMPLITUDE LOADING IN ASTM A514-B STEEL, ASTM STP536, 1973.

18. Fisher, J. W., Frank, K. H., Hirt, M. A. and McNamee, B. M.
EFFECT OF WELDMENTS ON THE FATIGUE STRENGTH OF STEEL BEAMS, NCRHP Report No. 102, Highway Research Board, National Academy of Sciences - National Research Council, Washington, D.C., 1970.

19. Miner, M. A.
CUMULATIVE DAMAGE IN FATIGUE, Journal of the Applied Mechanics, Vol. 12, No. 1, September 1945.

20. Schilling, C. G., Klippstein, K. H., Barsom, J. M. and Blake, G. T.
FATIGUE OF WELDED STEEL BRIDGE MEMBERS UNDER VARIABLE AMPLITUDE LOADING, Research Results Digest No. 60, Highway Research Board, 1974.

APPENDIX A

CRACK DOCUMENTATION

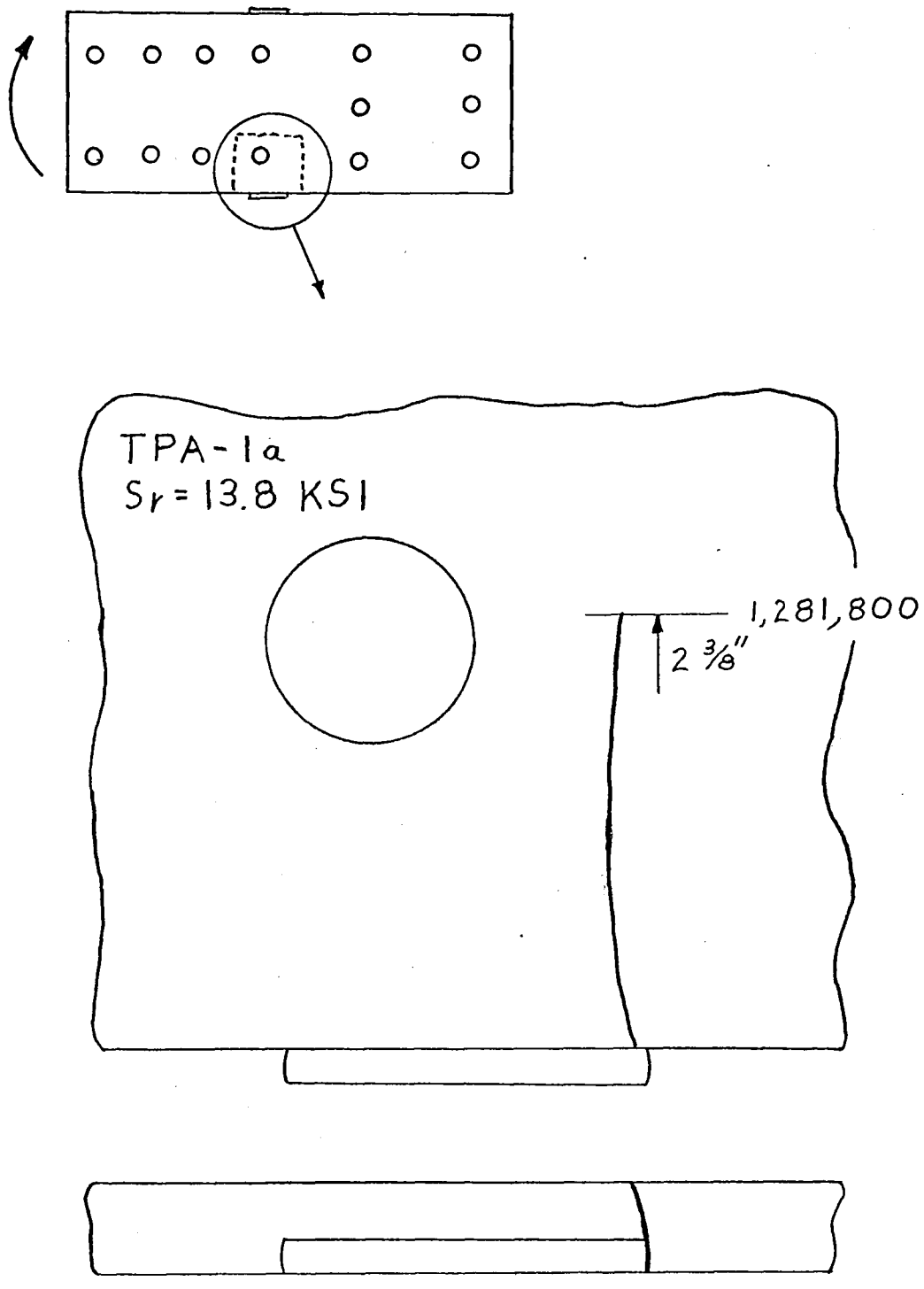

Fig. A-1 Tie Plate TPA-1a

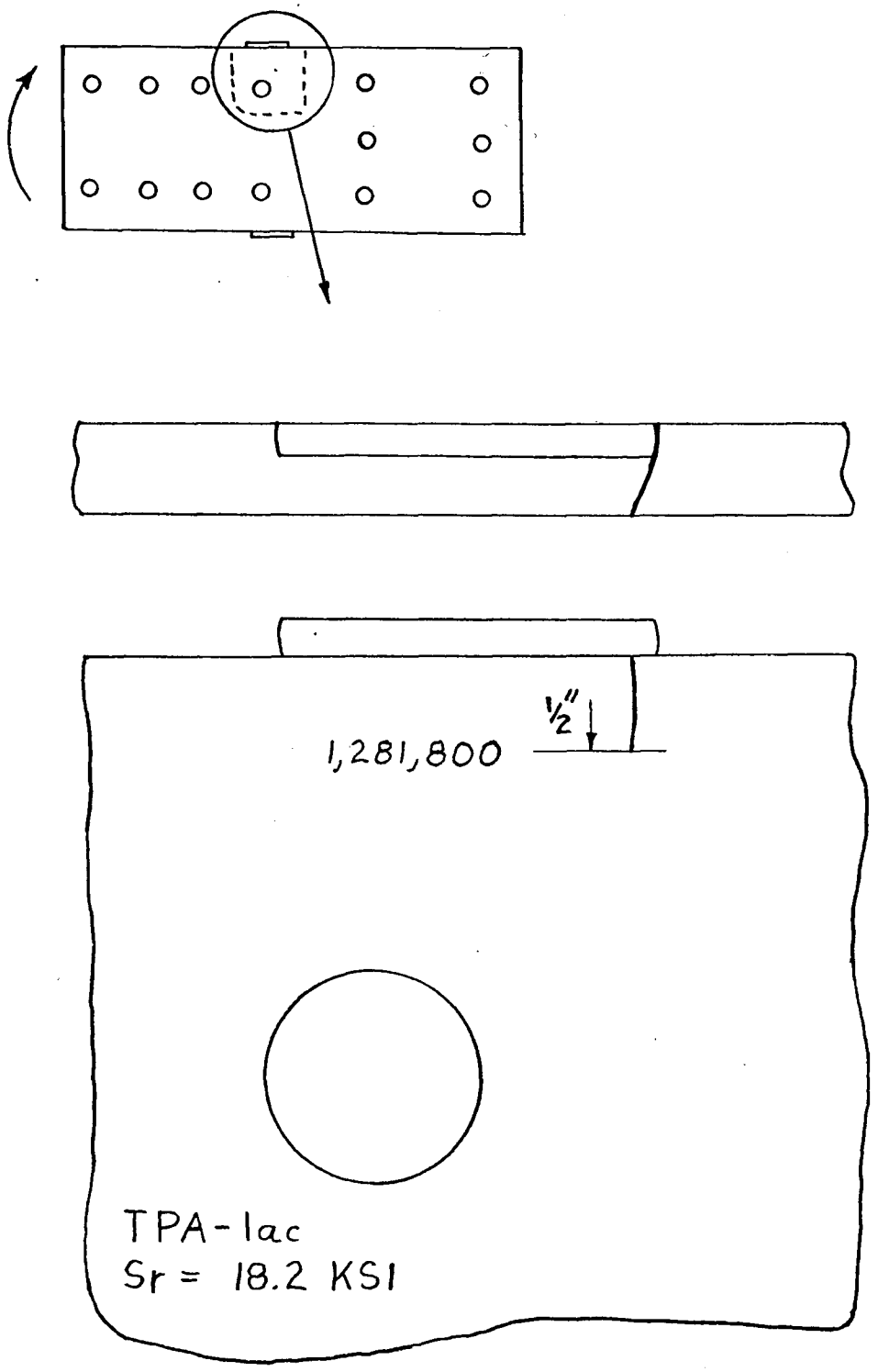

Fig. A-2 Tie Plate TPA-1ac

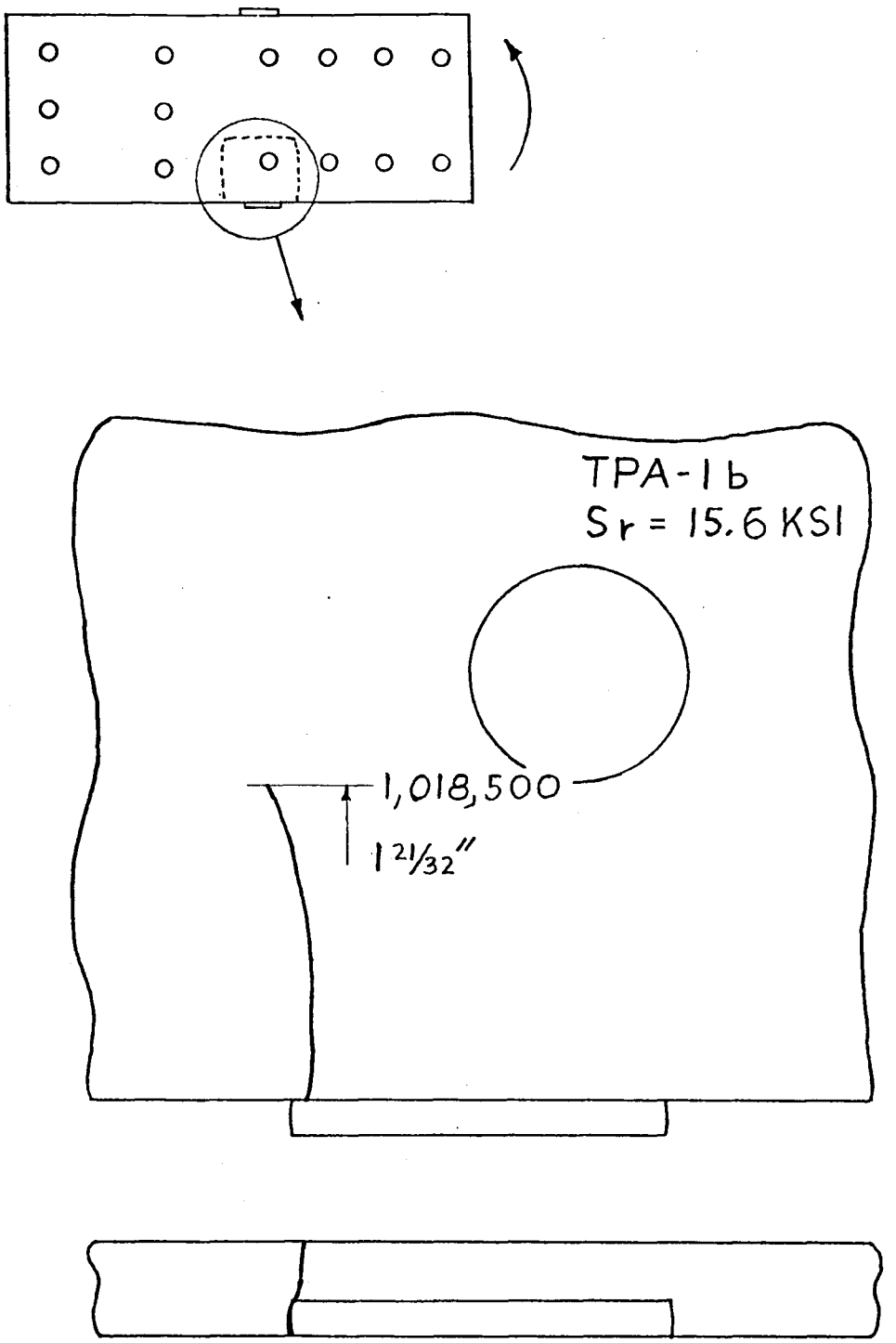

Fig. A-3 Tie Plate TPA-1b

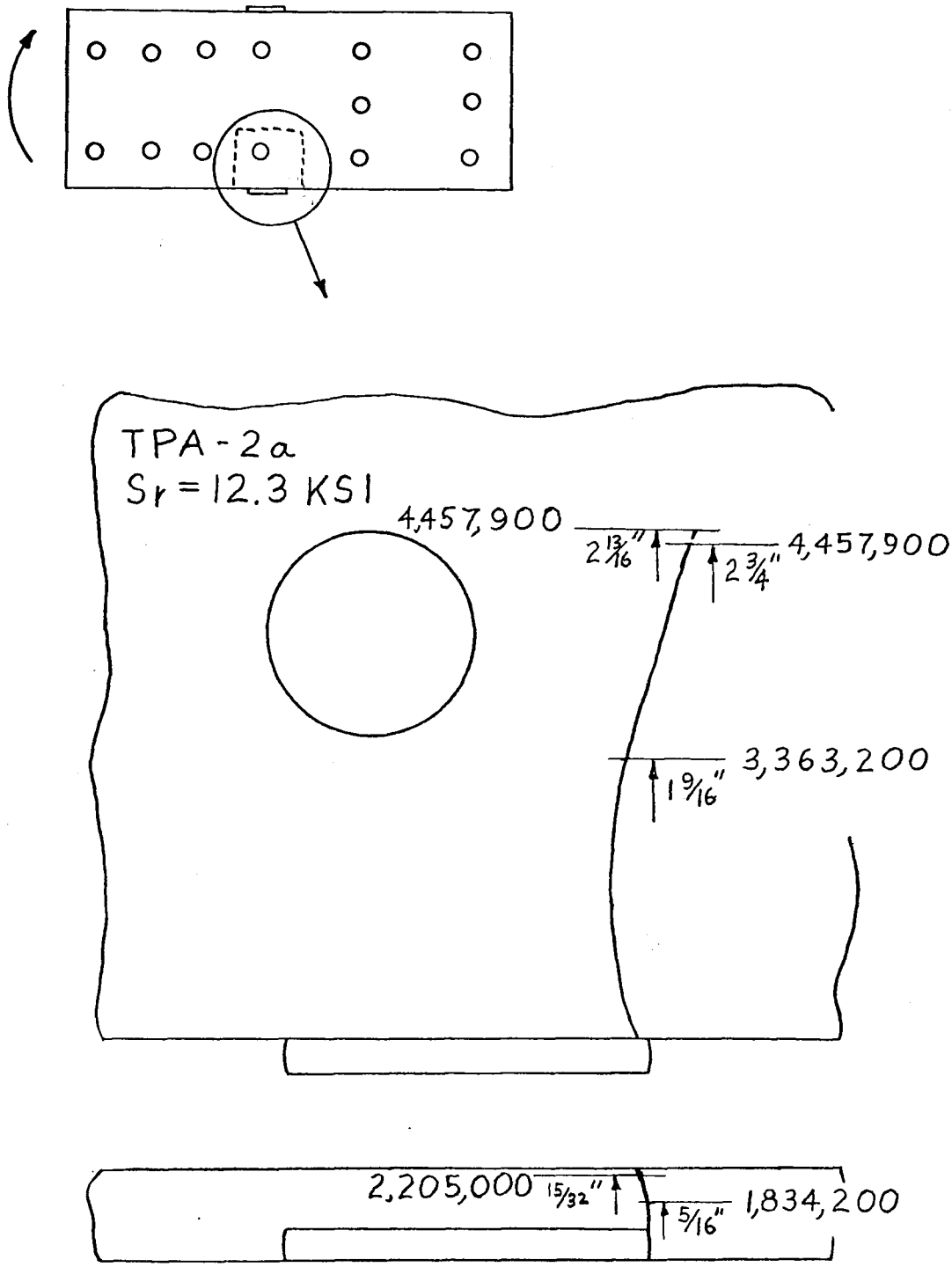

Fig. A-4 Tie Plate TPA-2a

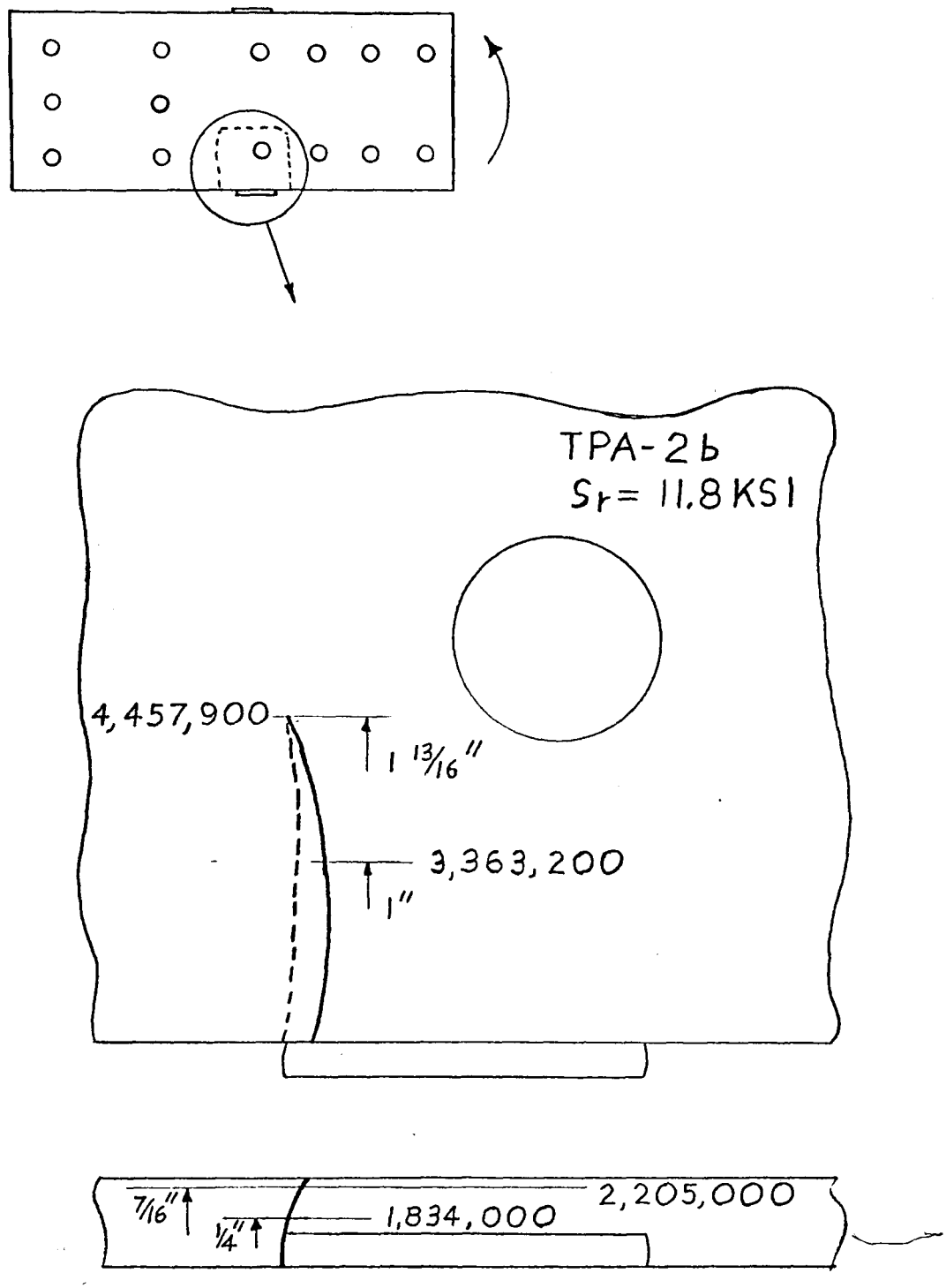

Fig. A-5 Tie Plate TPA-2b

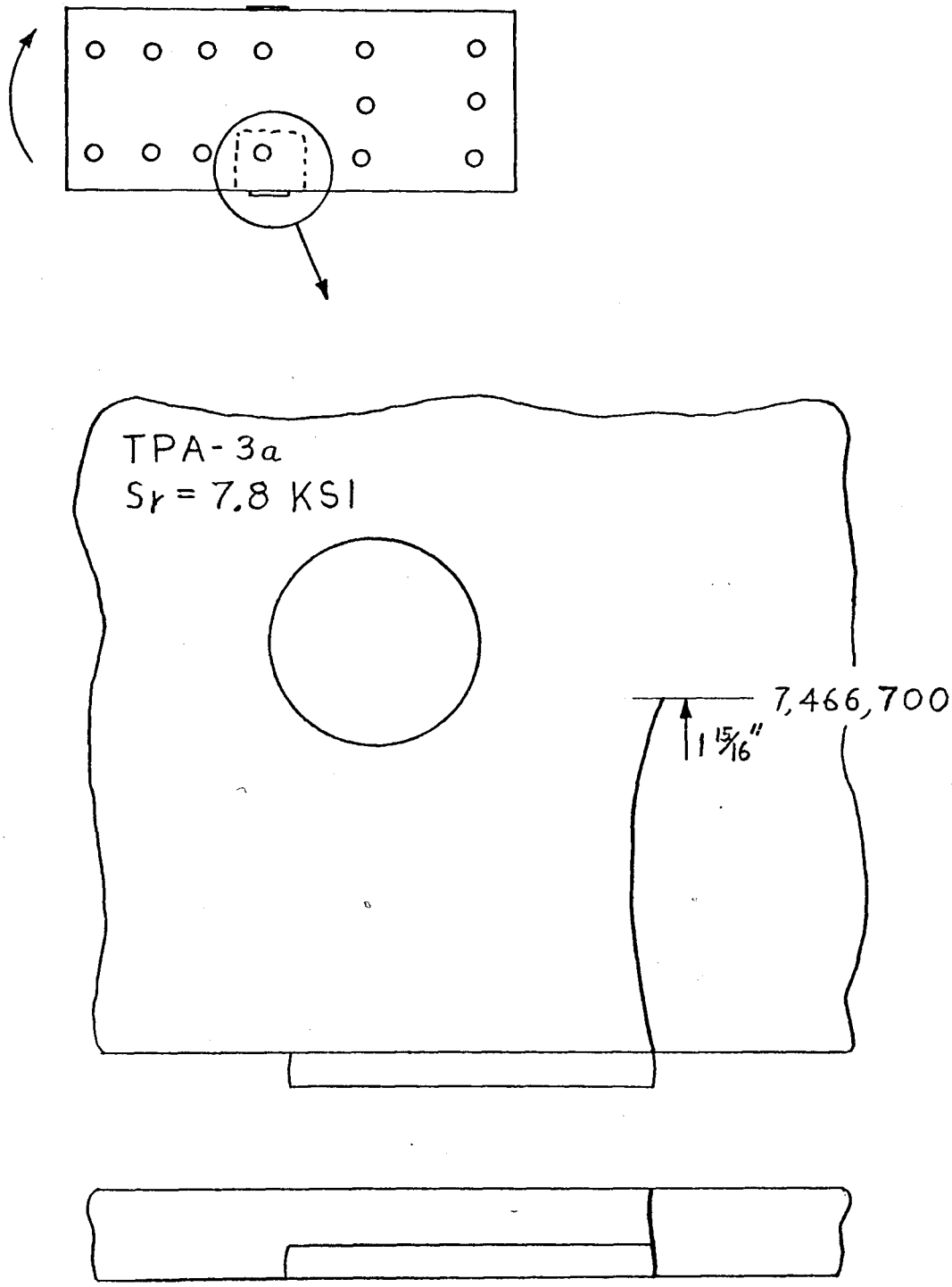

Fig. A-6 Tie Plate TPA-3a

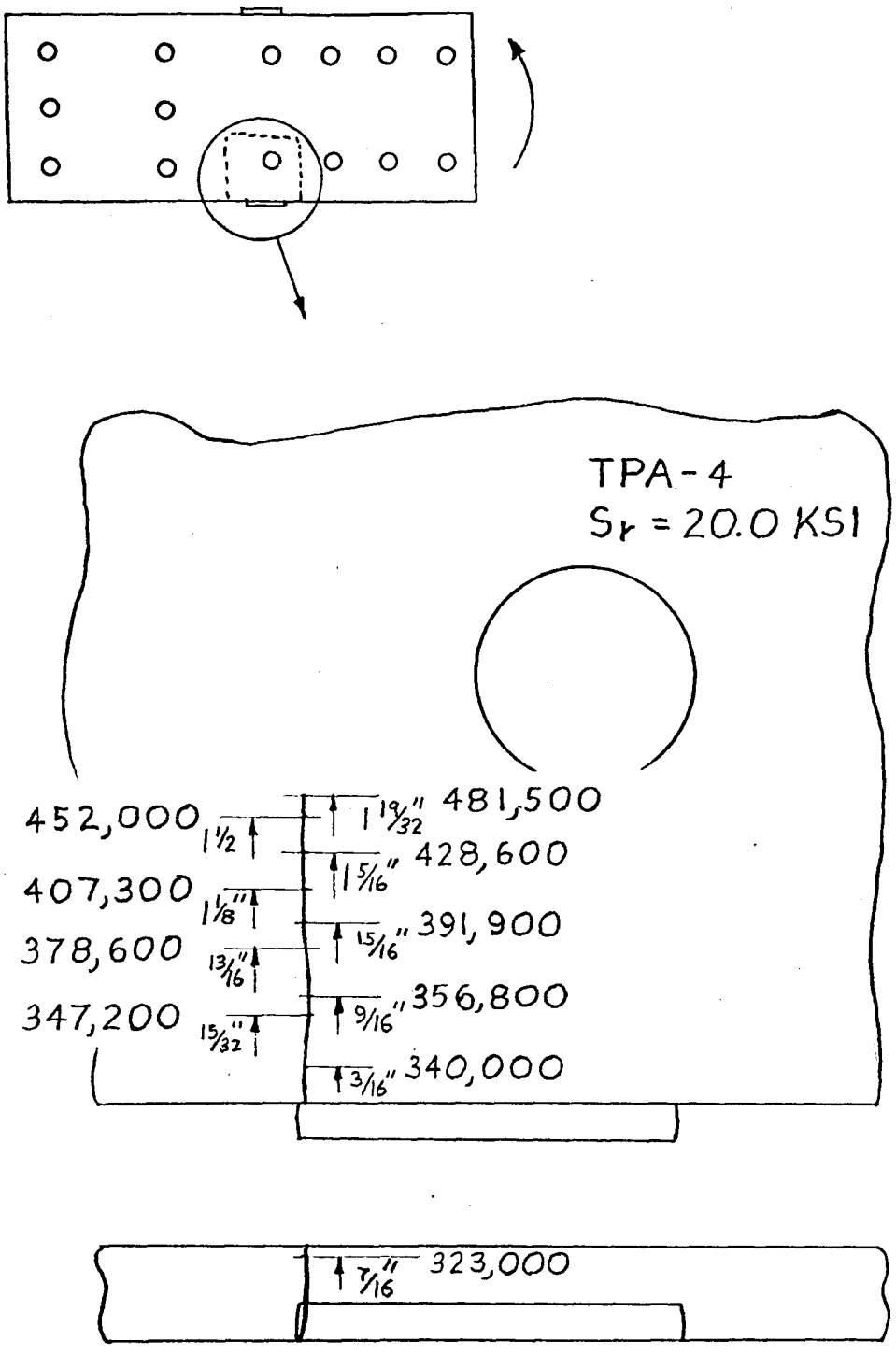

Fig. A-7 Tie Plate TPA-4

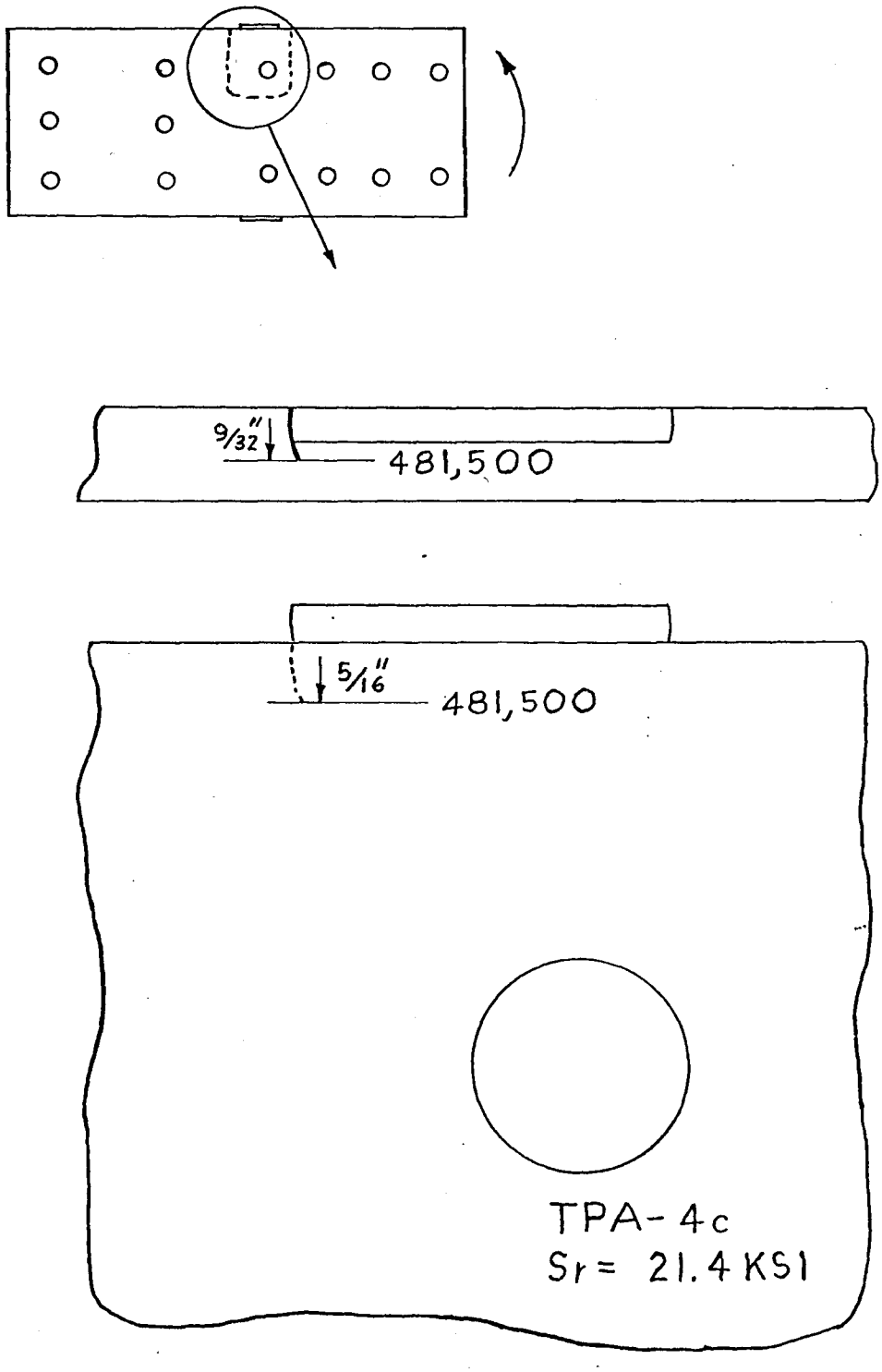

Fig. A-8 Tie Plate TPA-4c

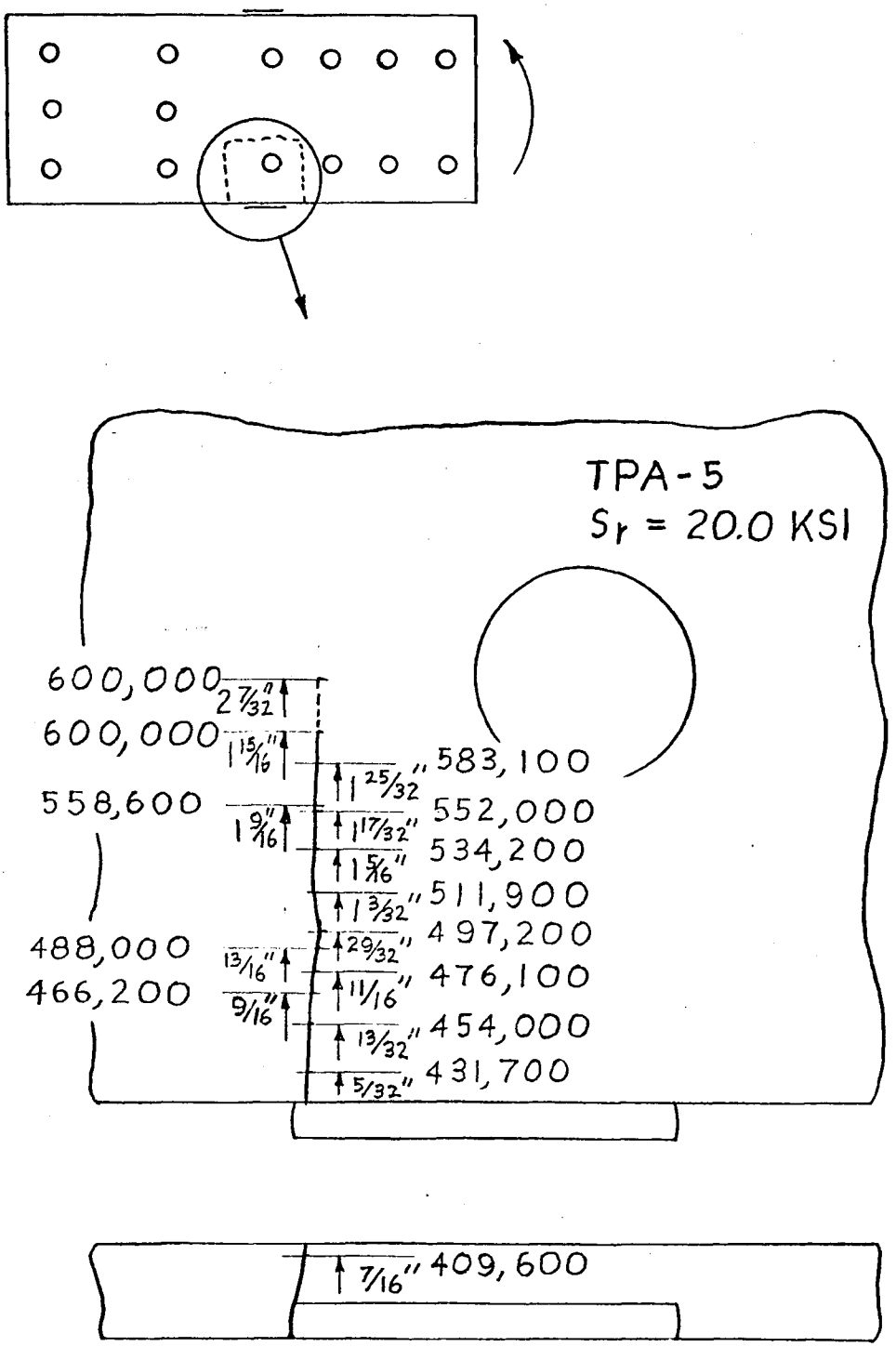

Fig. A-9 Tie Plate TPA-5

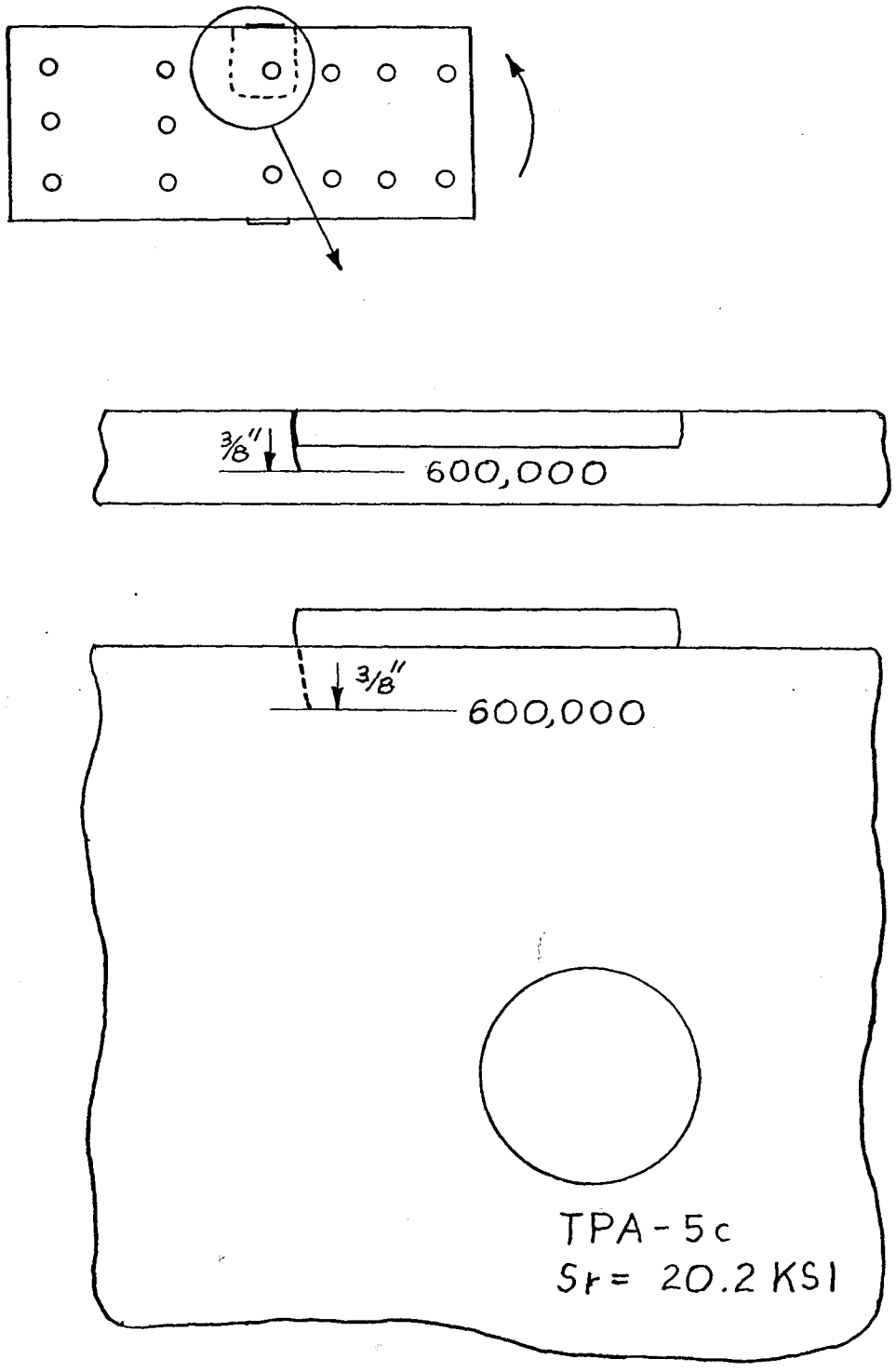

Fig. A-10 Tie Plate TPA-5c

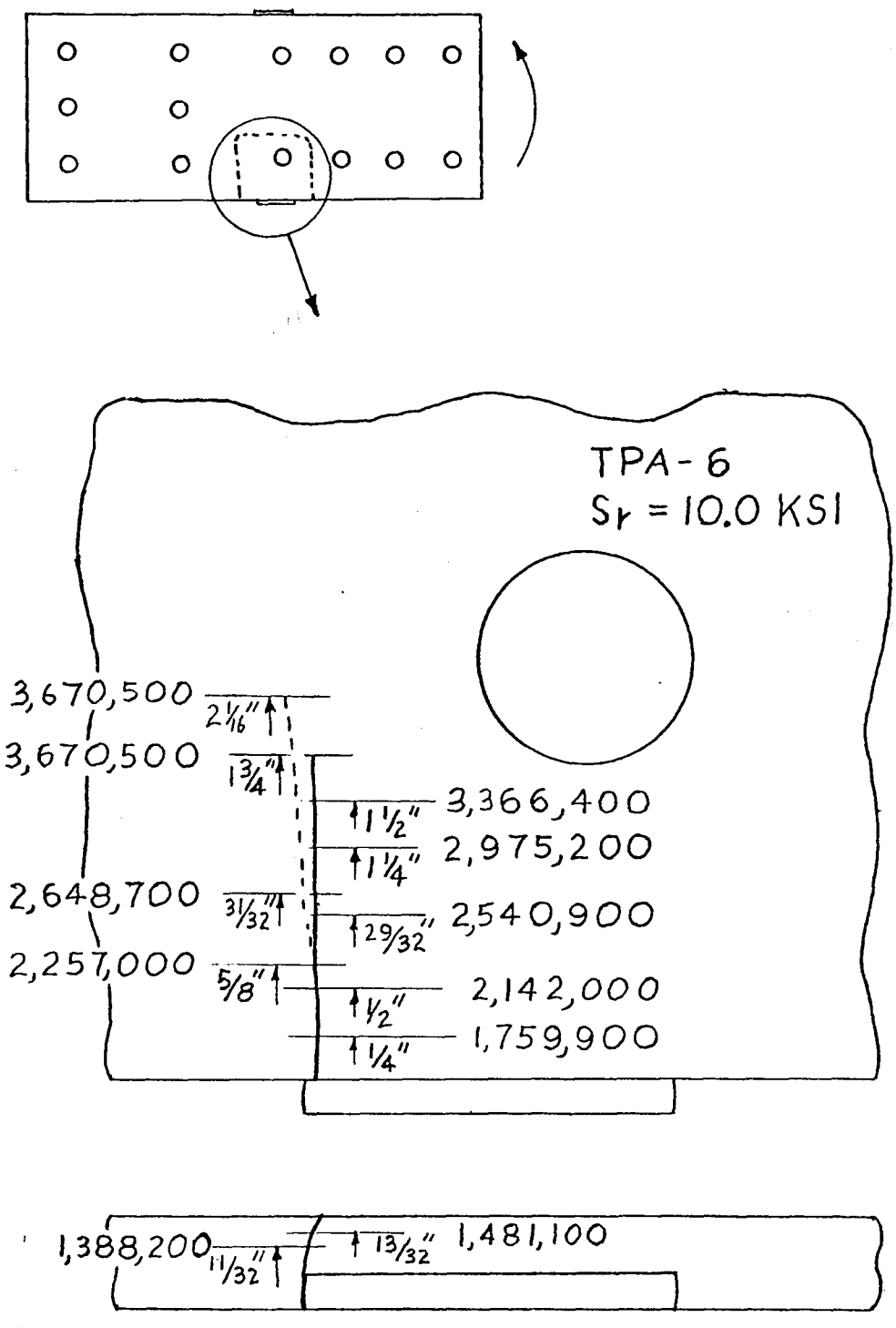

Fig. A-11 Tie Plate TPA-6

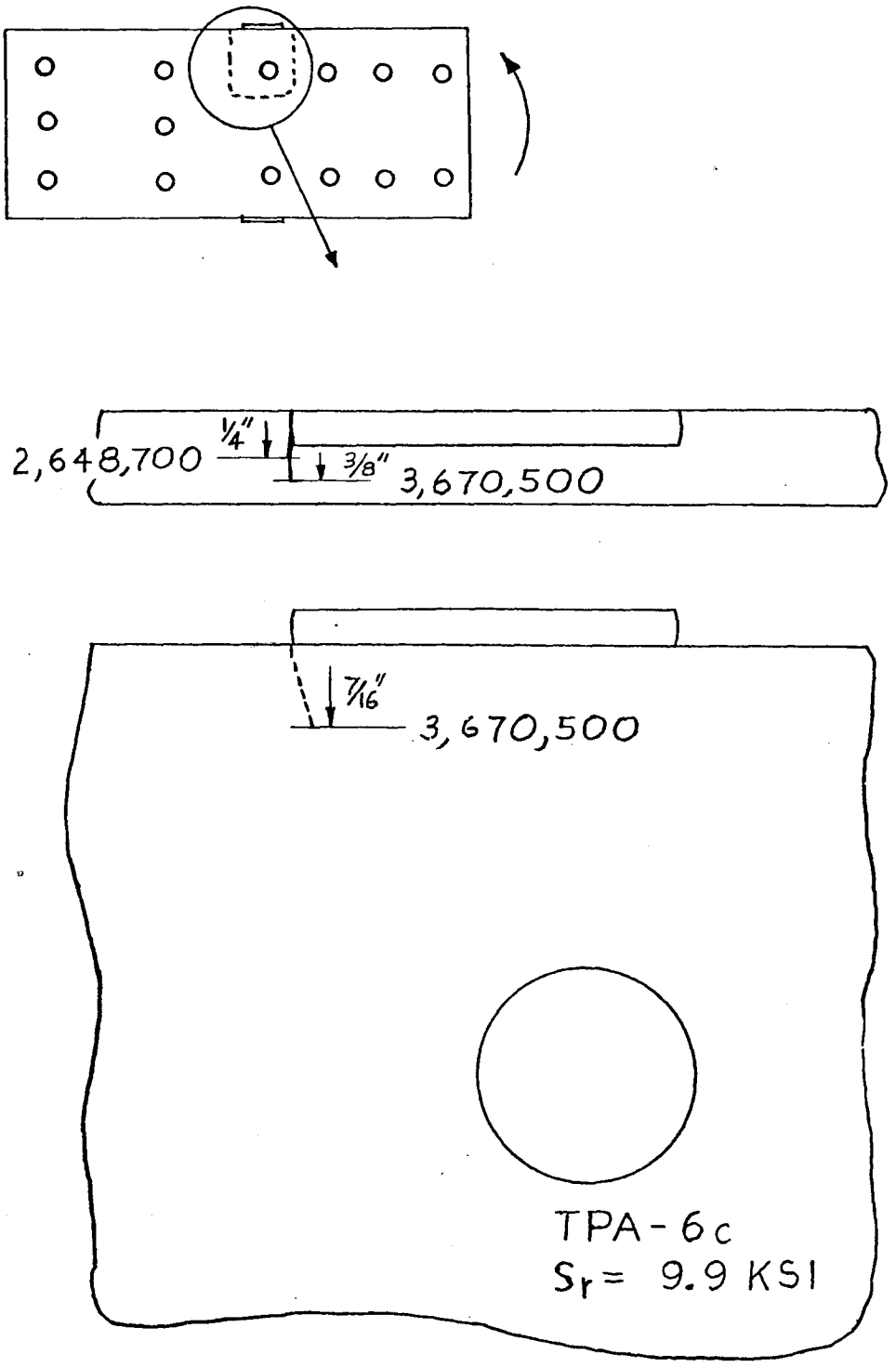

Fig. A-12 Tie Plate TPA-6c

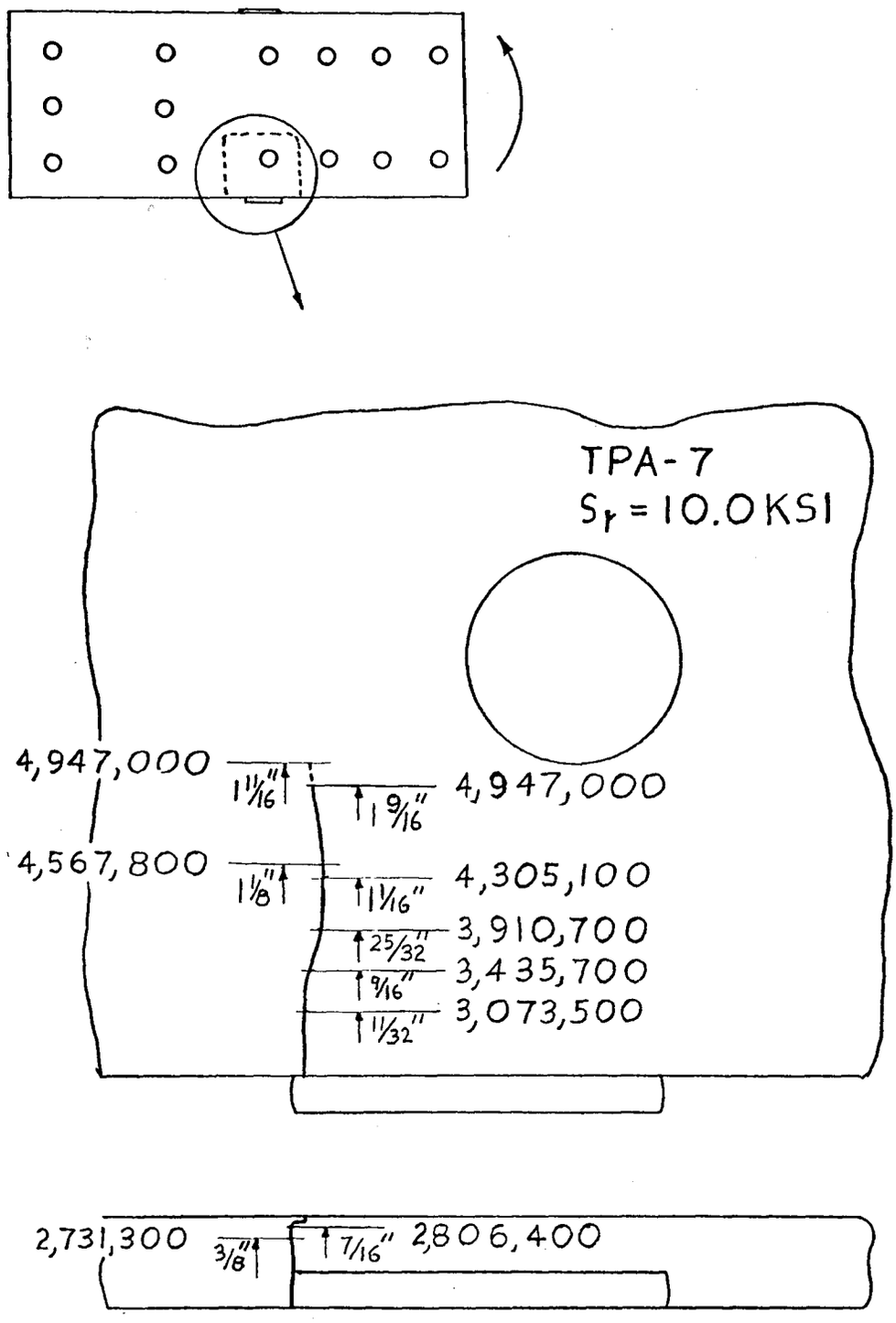

Fig. A-13 Tie Plate TPA-7

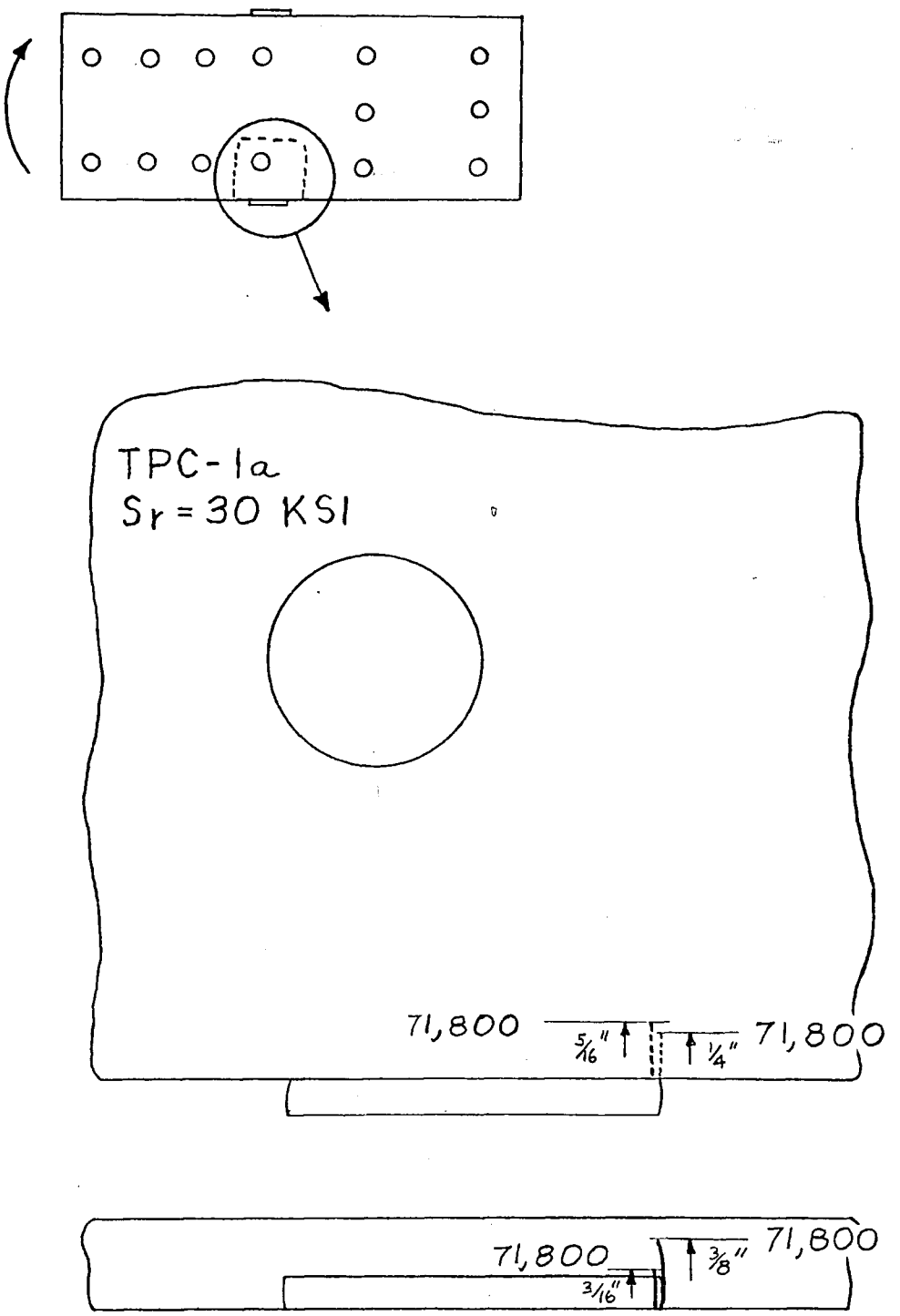

Fig. A-14 Tie Plate TPC-1a

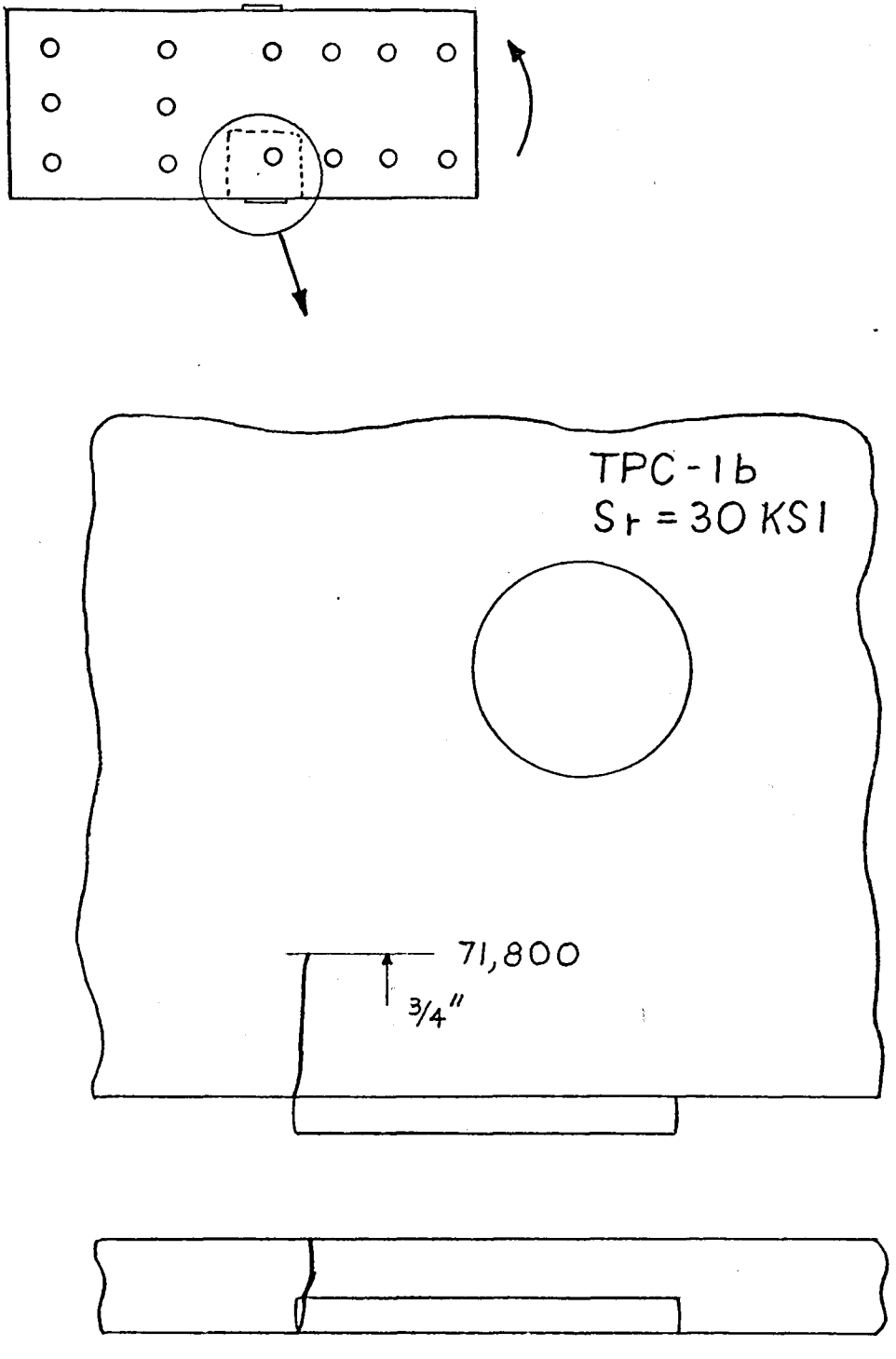

Fig. A-15 Tie Plate TPC-1b

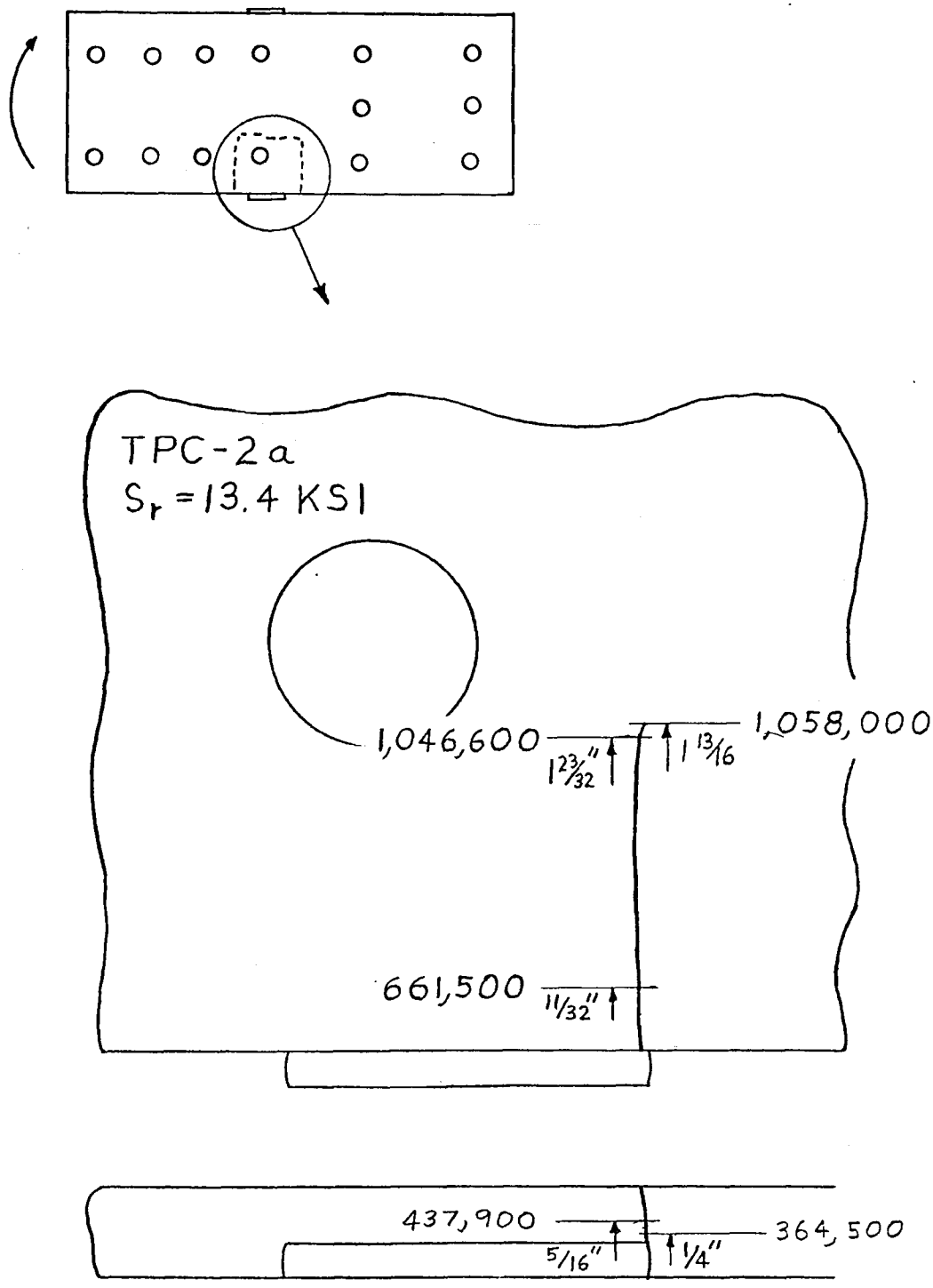

Fig. A-16 Tie Plate TPC-2a

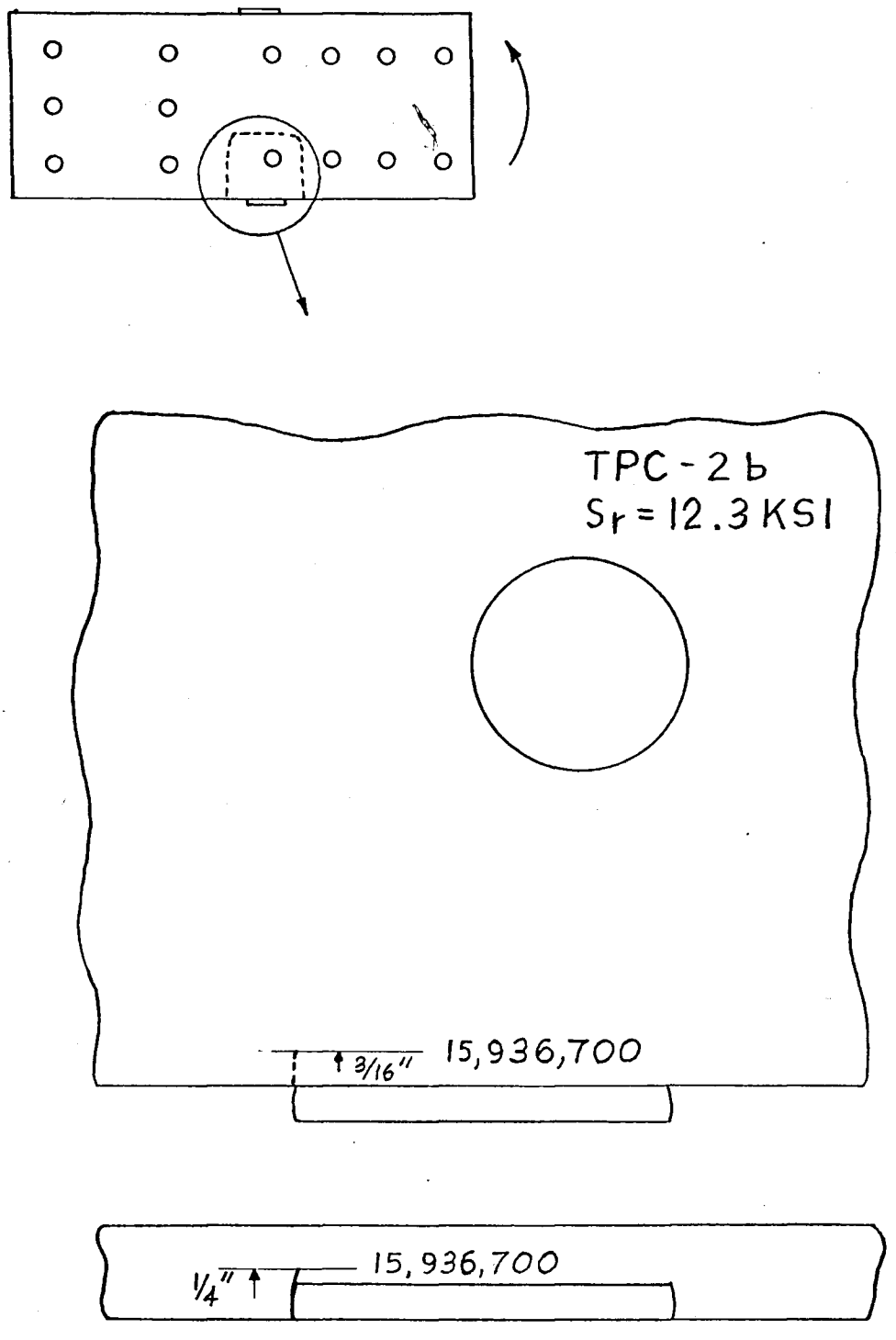

Fig. A-17 Tie Plate TPC-2b

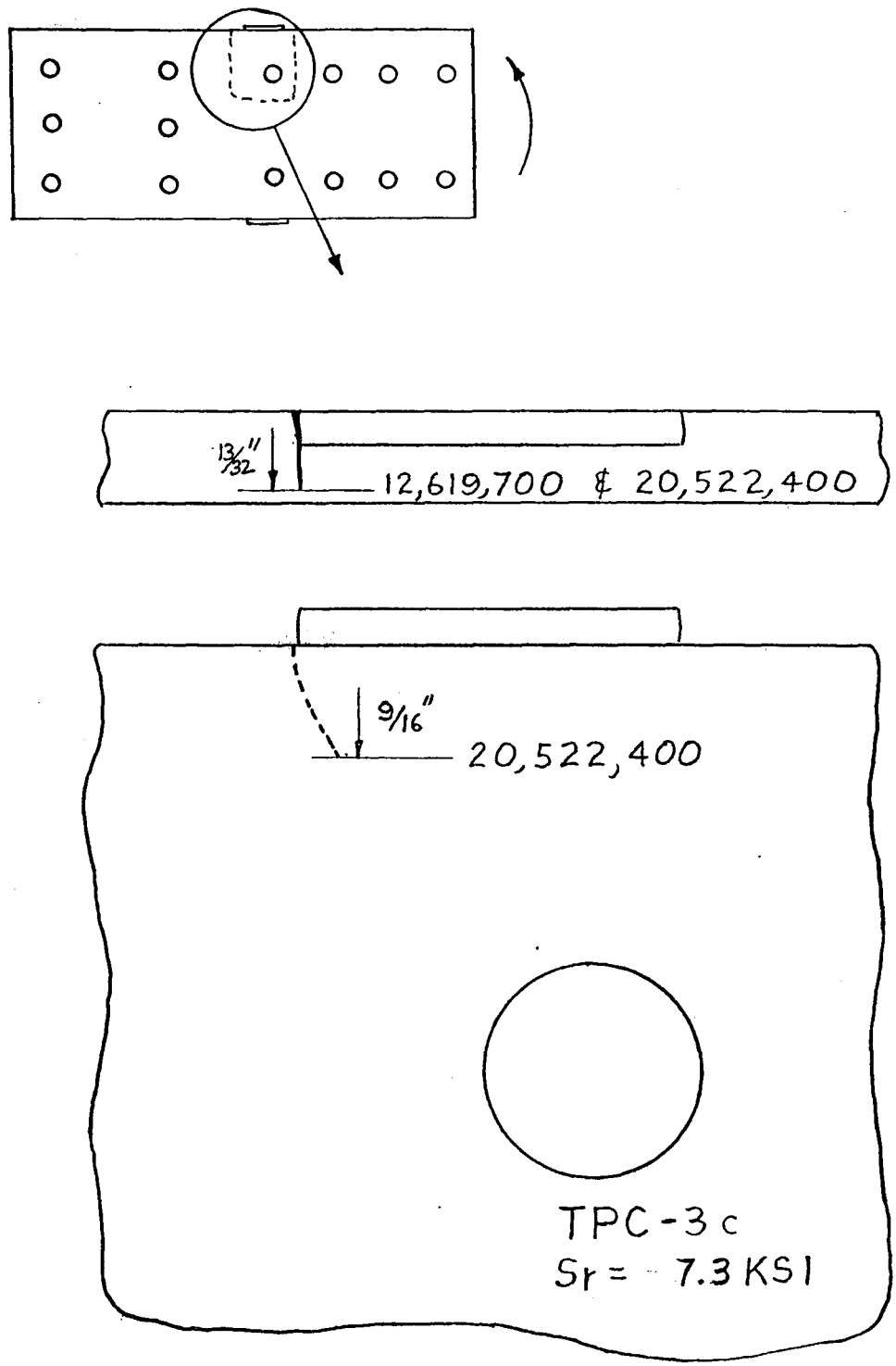

Fig. A-18 Tie Plate TPC-3c

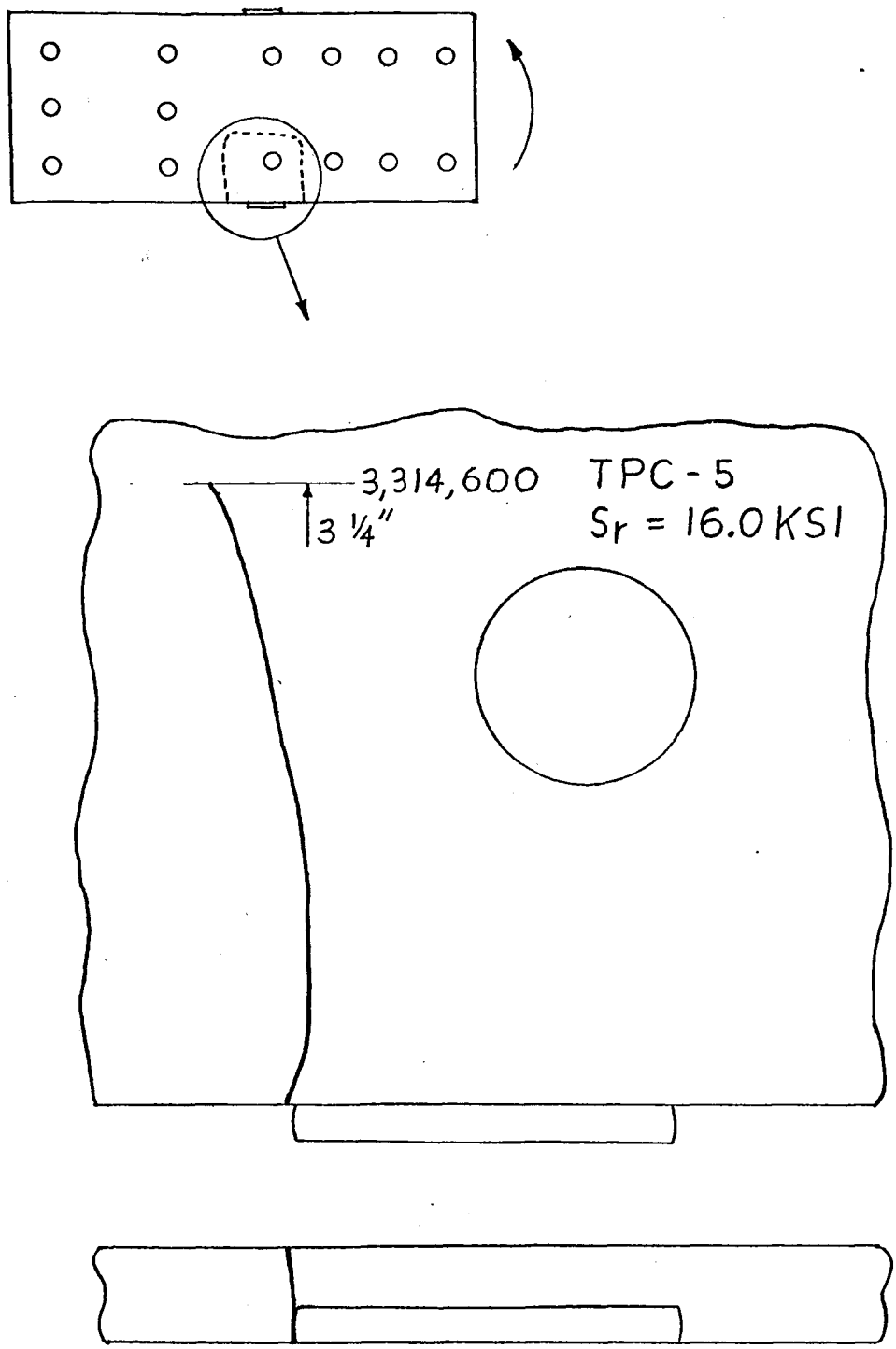

Fig. A-19 Tie Plate TPC-5

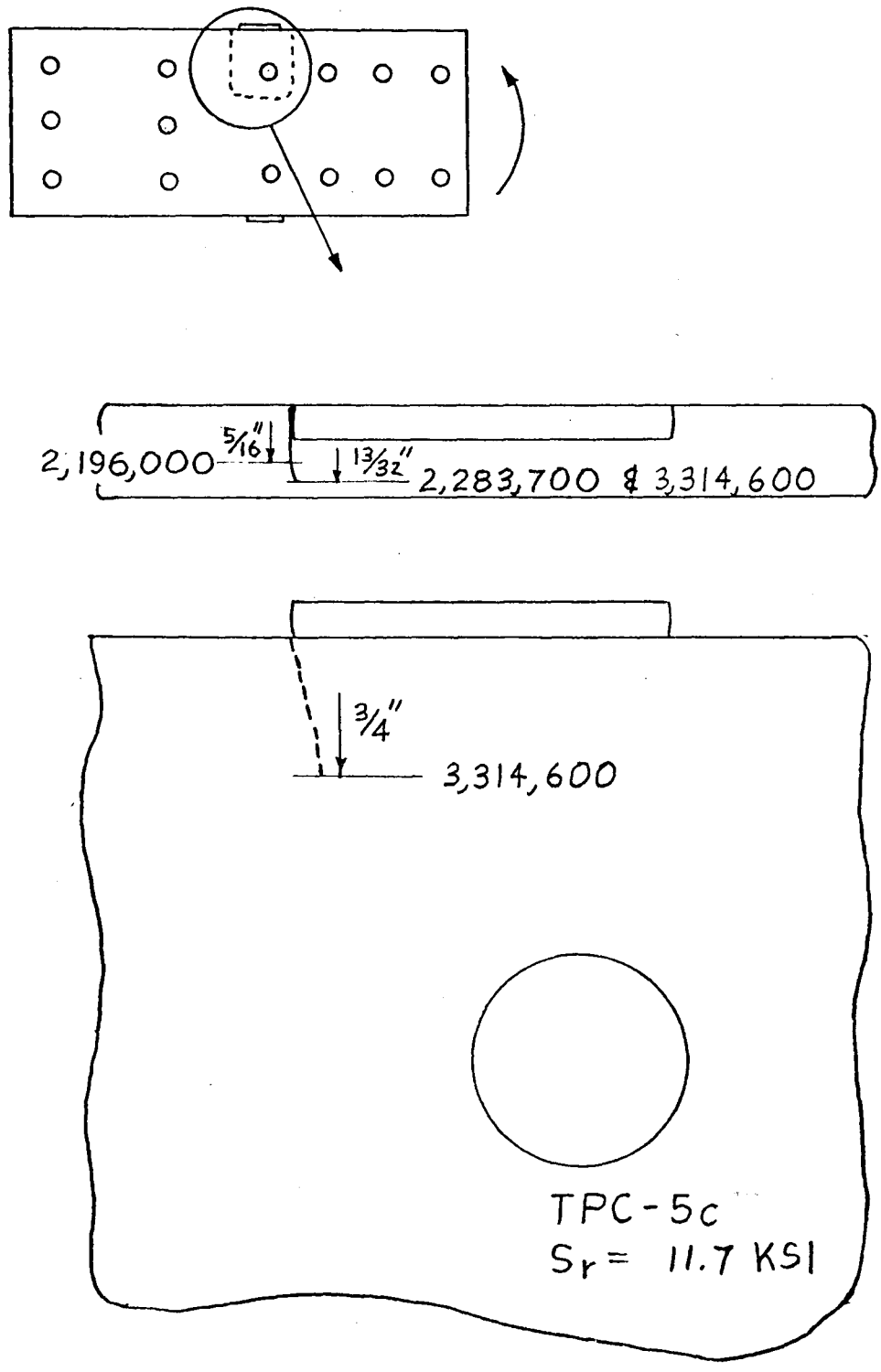

Fig. A-20 Tie Plate TPC-5c

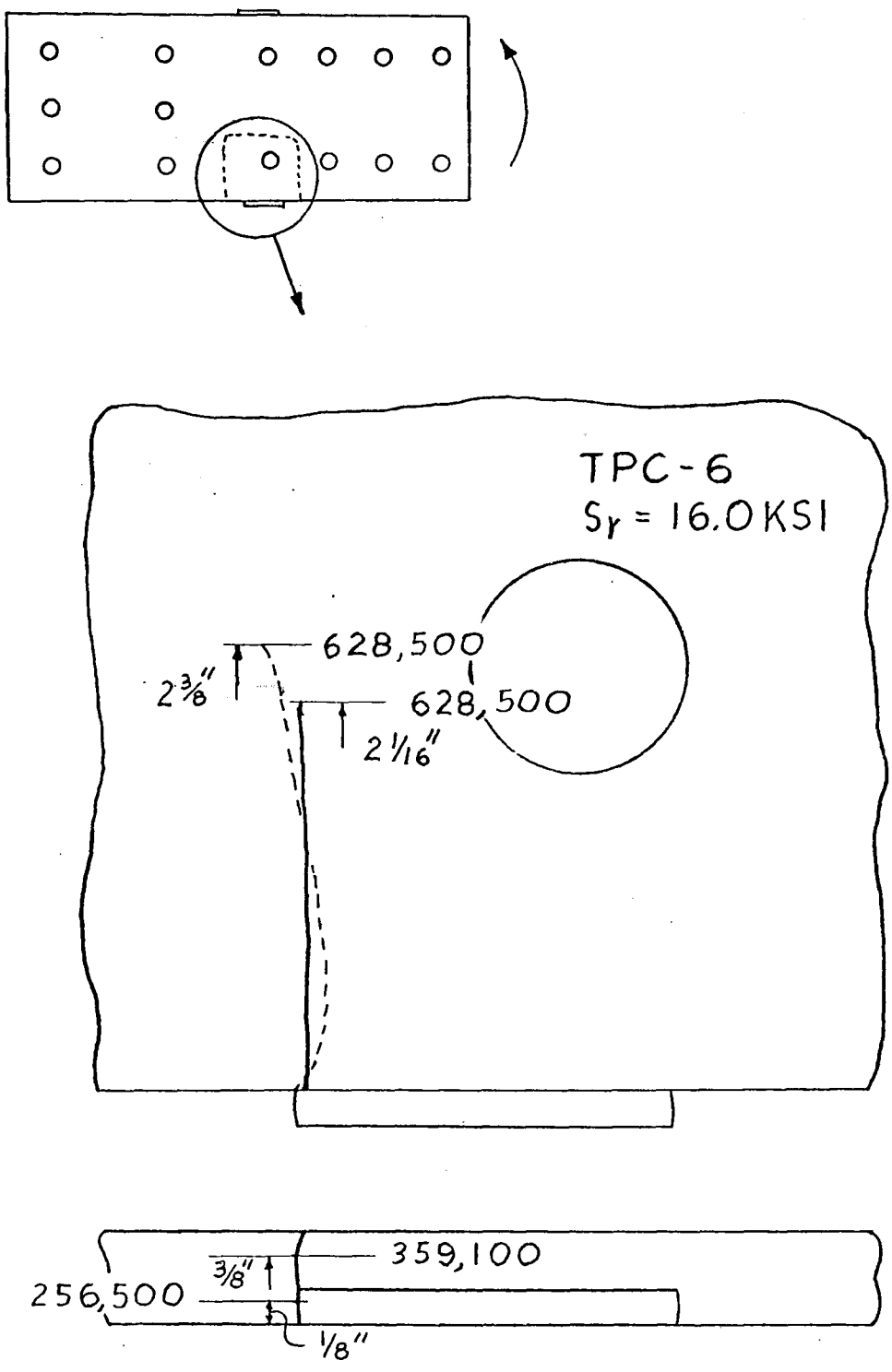

Fig. A-21 Tie Plate TPC-6

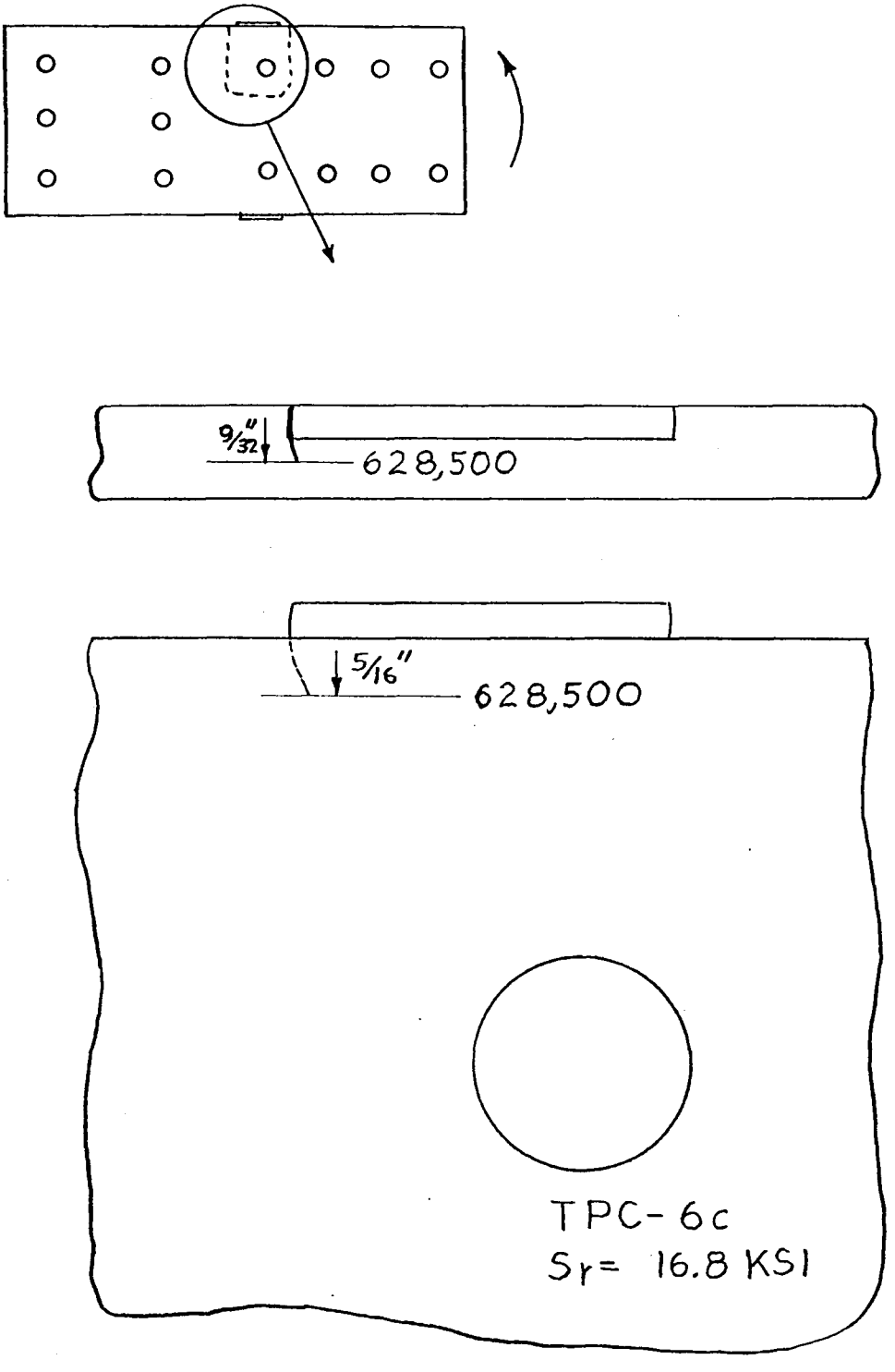

Fig. A-22 Tie Plate TPC-6c

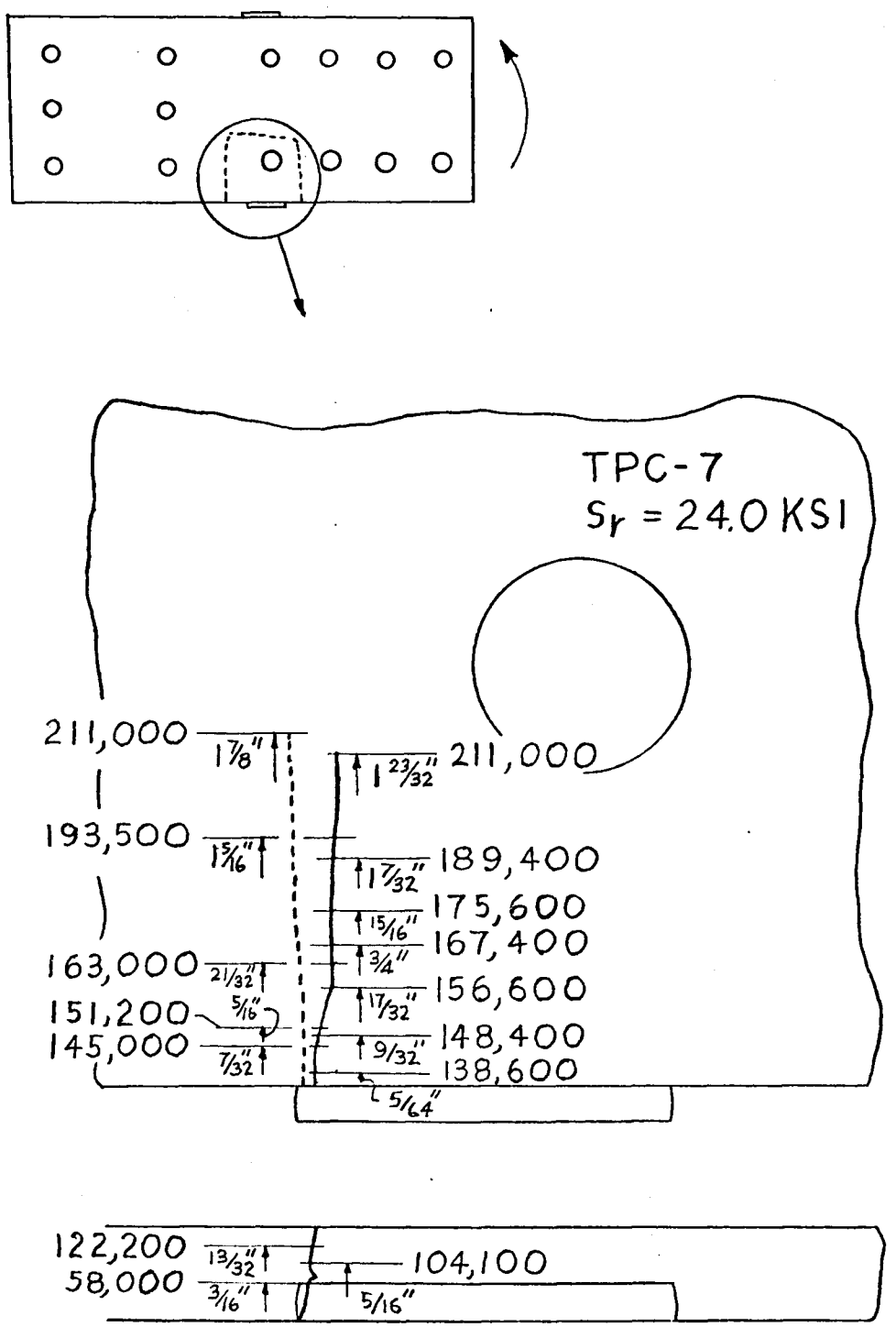

Fig. A-23 Tie Plate TPC-7

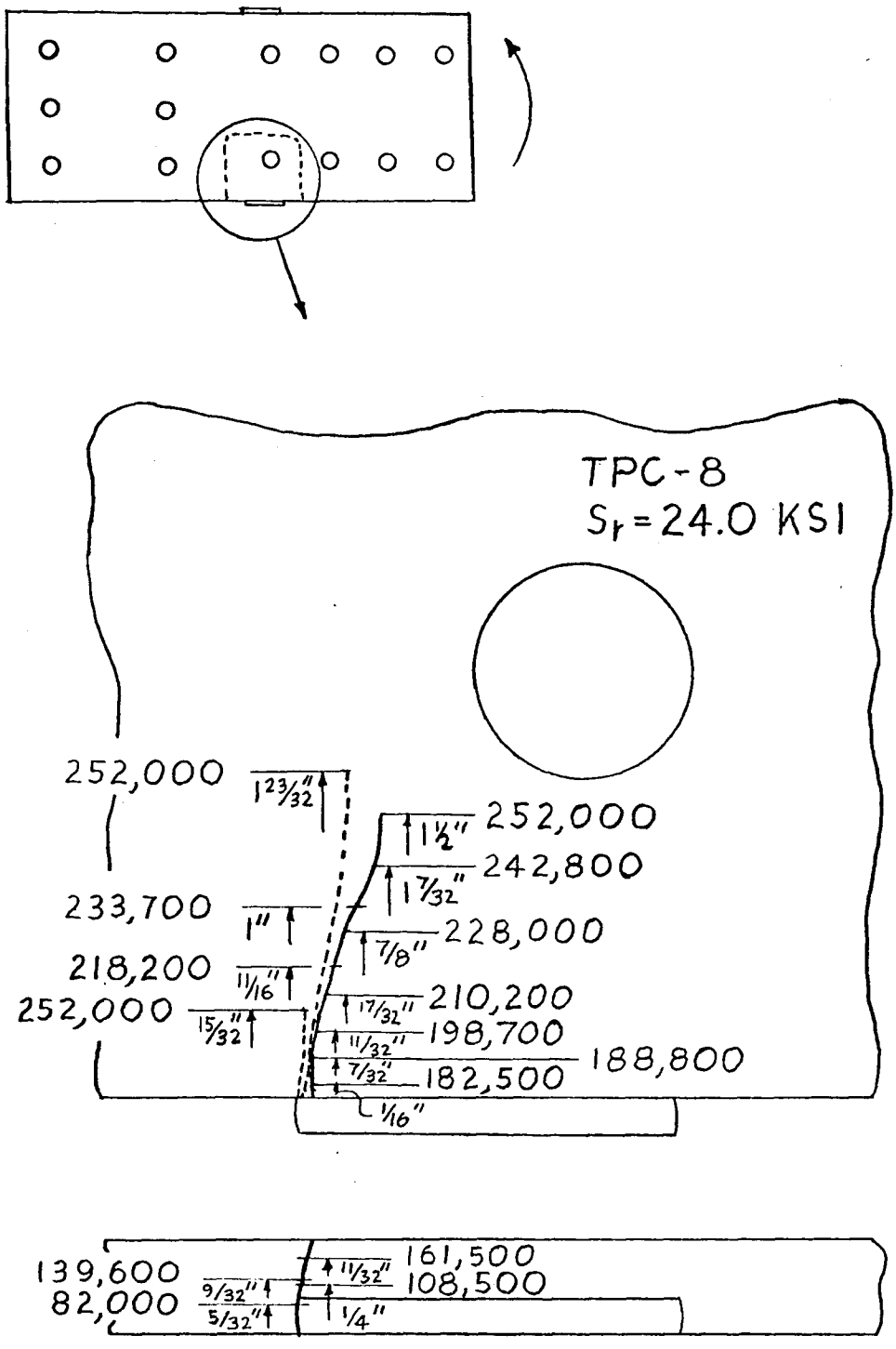

Fig. A-24 Tie Plate TPC-8

APPENDIX B

FATIGUE CRACKING OF THE UNWELDED TIE PLATE

Near the end of the tie plate test the unwelded tie plate on the east side of the test set-up developed a fatigue crack. The crack started at the bottom hole under a washer and was not discovered until it had grown 8-1/8 in. This crack is shown schematically in Fig. B-1.

The bolted connection was not fully slip resistant since the bolts were only preloaded between 20-25 kips, which is less than the full clamping force of 1 in. A490 high strength bolts. Previous tests have shown that reducing the clamping force lowers the fatigue life of a bolted joint[13,14]. Therefore this failure was compared to Category B of the AASHTO Specification[4] for a bearing-type joint. Since the fatigue strength of bearing joints are governed by stresses on the net section, all calculated stresses on the unwelded tie plate were based on bending stresses at the net section.

Category B was derived from fatigue data for welded details and shown to provide a lower bound to the fatigue strength of bolted bearing joints with fully preloaded joints[14]. A lower bound estimate of the fatigue crack growth threshold for bolts with low clamping force was made using a linear approximation of the stress intensity factor for a small crack at the edge of a hole[15]. Since the tie plate holes were drilled, a small initial crack (a_i) of 0.005 in. was assumed. This resulted in the following approximation for the stress intensity factor

$$K = 2.97\ \sigma\ \sqrt{\pi a}\quad (\text{ksi}\ \sqrt{\text{in}}\ ) \tag{B-1}$$

where σ is the stress based on the gross area. Dividing this stress by the ratio of net area to gross area gives the stress based on the net section, which is needed for this analysis. By substituting a rounded value of the stress intensity range threshold found by Klingerman[11] of 3.0 ksi $\sqrt{\text{in.}}$ into Eq. B-1 for K, along with 0.005 in. for a and the correction for stress based on net section, a threshold stress range of 10 ksi was estimated for the tie plate.

A strain gage had been placed on the tie plate's bottom edge to check twisting of the beam. Therefore the stress range at the edge of the hole could be estimated for each block of loading. The resulting stress ranges and cycle history is summarized in Table B-1.

The root-mean-square (RMS) method[16,17,18] was one of two procedures used to determine an effective stress range so that the failure could be compared with the constant cycle relationship. In this method the root-mean-square stress range is defined as:

$$S_{rRMS} = \left(\Sigma\ \alpha_i\ S_{r_i}^2\right)^{1/2} \tag{B-2}$$

where α_i is the frequency of occurrence of stress range S_{r_i}.

The second procedure consisted of combining the relationship provided by constant cycle data[18] and Miner's cumulative damage hypothesis[19] to obtain an equivalent stress range S_{rMiner}[20]. This equivalent stress range was estimated as

$$S_{rMiner} = \left(\Sigma \alpha_i S_{r_i}^3 \right)^{1/3} \qquad \text{(B-3)}$$

where α_i is the frequency of occurrence of stress range S_{r_i}.

In order to assess the most critical condition, several effective stress range values were determined for the random block loading sequence. Several of the initial block loadings were below the fatigue limit of 10 ksi. Hence the lower stress range blocks were eliminated from the effective stress range analysis one at a time. The results of this analysis are tabulated in Table B-2 and plotted along with Category B in Fig. B-2. Since there may not be a fatigue limit for random cyclic loading when some of the stress cycles exceed the fatigue limit this figure shows the stress range-cycle life relationship extended beyond the fatigue limit.

The first block loading (TPC-3) with a 6.5 ksi stress range can logically be eliminated from the effective stress calculation, since it was well below the threshold. The second block eliminated was TPA-7 with a stress range of 7.1 ksi. Although some crack growth may have occurred under earlier loading blocks, it is probable that the crack size did not increase enough to cause the crack growth threshold to be exceeded at a 7.1 ksi stress range. This same reasoning was used to eliminate the 7.8 ksi stress range of the third block loading, TPA-6. The 11.3 and 13.3 ksi stress ranges of TPC-5 and TPC-6 respectively were also eliminated to determine the effects on the fatigue strength calculations.

Figure B-2 shows that removing up to three of the lower stress range blocks provided approximately the same tie plate fatigue strength. The test data fall at or above the stress range-cycle life relationship for Category B indicating failure. When more stress range blocks were truncated the effective stress range began to fall below the fatigue strength line indicating that no failure should occur. Therefore any one of the first four effective stress ranges calculated gives a reasonable estimate of the tie plate's fatigue strength.

TABLE B-1 UNWELDED TIE PLATE STRESS RANGE AND CYCLE HISTORY

Specimen	Cycles	Stress Range (S_r) at Hole, Base on Net Section (ksi)
TPC-3	20,522,400	6.5
TPC-5	3,314,600	11.3
TPA-6	3,670,500	7.8
TPC-6	628,500	13.3
TPA-7	4,947,000	7.1
TPA-4	481,500	16.9
TPC-7	211,000	17.4
TPC-8	252,000	18.7
TPA-8	1,582,000	13.5

NOTE: 1. Specimens listed in order of testing

2. TPA-8 not included in S-N curve as results questionable because of crack in unwelded tie plate

TABLE B-2 SUMMARY OF EFFECTIVE STRESS RANGES

Specimens Excluded	Total Cycles	$S_{r_{RMS}}$ (ksi)	$S_{r_{MINER}}$ (ksi)
None	35,609,500	8.3	8.8
TPC-3	15,087,100	10.3	10.8
TPC-3 TPA-7	10,140,100	11.5	12.2
TPC-3 TPA-7 TPA-6	6,469,600	13.1	13.3
TPC-3 TPA-7 TPA-6 TPC-5	3,155,000	14.8	14.9
TPC-3 TPC-7 TPA-6 TPC-5 TPC-6	2,526,500	15.1	15.3

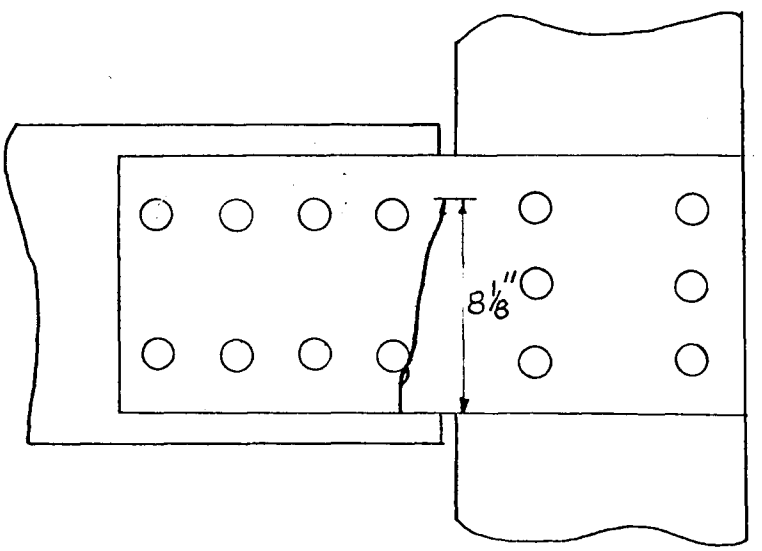

Fig. B-1 Schematic of Fagiue Crack in Unwelded Tie Plate

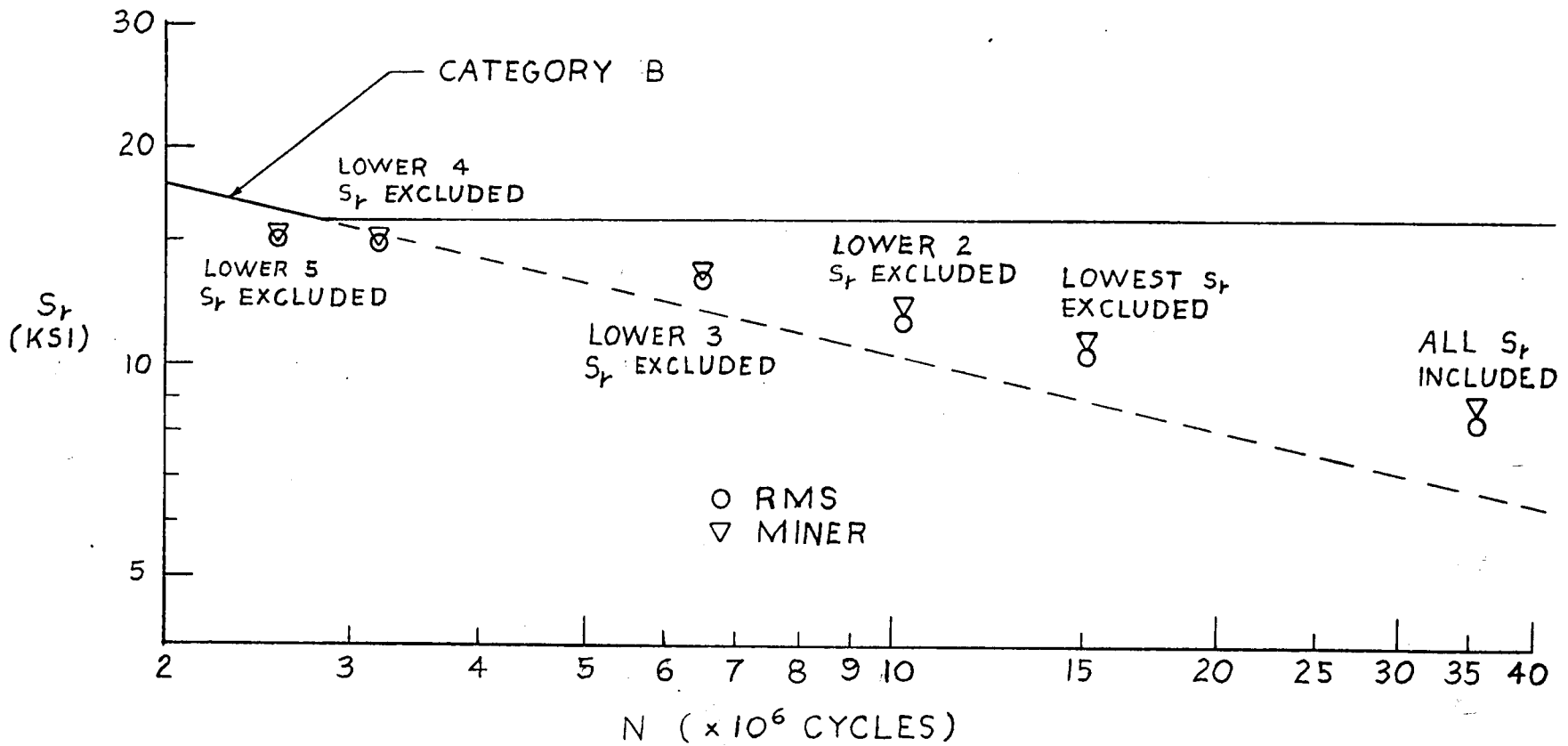

Fig. B-2 Unwelded Tie Plate Fatigue Failure Compared to Category B

VITA

Donald P. Erb, the son of Katharine and Paul S. Erb, was born on October 16, 1950 in Lancaster, Pennsylvania. The author attended Manheim Township High School in Lancaster. He was a Dean's List student at Drexel University in Philadelphia, Pennsylvania where he received a Bachelor of Science degree in Civil Engineering with highest honors in June, 1973. He was awarded a Research Assistantship in Civil Engineering at Fritz Engineering Laboratory, Lehigh University in October, 1973 and received his Master of Science degree in Civil Engineering from Lehigh University in October, 1975.